

670295

DP-MS-83-27, Rev. 1

**2-D SIMULATIONS OF DRAINAGE WINDS AND DIFFUSION
COMPARED TO OBSERVATIONS**

by

Alfred J. Garrett and Frank G. Smith, III

Savannah River Laboratory
E. I. du Pont de Nemours & Co.
Aiken, SC 29808

December 8, 1983

SRL
RECORD COPY

For publication in
Journal of Climate and Applied Meteorology

This paper was prepared in connection with work done under Contract No. DE-AC09-76SR00001 with the U.S. Department of Energy. By acceptance of this paper, the publisher and/or recipient acknowledges the U.S. Government's right to retain a nonexclusive, royalty-free license in and to any copyright covering this paper, along with the right to reproduce and to authorize others to reproduce all or part of the copyrighted paper.

This document was prepared in conjunction with work accomplished under Contract No. DE-AC09-76SR00001 with the U.S. Department of Energy.

DISCLAIMER

This report was prepared as an account of work sponsored by an agency of the United States Government. Neither the United States Government nor any agency thereof, nor any of their employees, makes any warranty, express or implied, or assumes any legal liability or responsibility for the accuracy, completeness, or usefulness of any information, apparatus, product or process disclosed, or represents that its use would not infringe privately owned rights. Reference herein to any specific commercial product, process or service by trade name, trademark, manufacturer, or otherwise does not necessarily constitute or imply its endorsement, recommendation, or favoring by the United States Government or any agency thereof. The views and opinions of authors expressed herein do not necessarily state or reflect those of the United States Government or any agency thereof.

This report has been reproduced directly from the best available copy.

Available for sale to the public, in paper, from: U.S. Department of Commerce, National Technical Information Service, 5285 Port Royal Road, Springfield, VA 22161, phone: (800) 553-6847, fax: (703) 605-6900, email: orders@ntis.fedworld.gov online ordering: <http://www.ntis.gov/ordering.htm>

Available electronically at <http://www.doe.gov/bridge>

Available for a processing fee to U.S. Department of Energy and its contractors, in paper, from: U.S. Department of Energy, Office of Scientific and Technical Information, P.O. Box 62, Oak Ridge, TN 37831-0062, phone: (865) 576-8401, fax: (865) 576-5728, email: reports@adonis.osti.gov

**2-D SIMULATIONS OF DRAINAGE WINDS AND DIFFUSION
COMPARED TO OBSERVATIONS**

by

Alfred J. Garrett and Frank G. Smith, III

Savannah River Laboratory
E. I. du Pont de Nemours & Co.
Aiken, SC 29808

ABSTRACT

A vertically integrated dynamical drainage flow model is developed from conservation equations for momentum and mass in a terrain-following coordinate system. Winds fields from the dynamical model drive a Monte Carlo transport and diffusion model. The model needs only topographic data, an Eulerian or Lagrangian time scale and a surface drag coefficient for input data, and can be started with a motionless atmosphere. Model wind and diffusion predictions are compared to observations from the rugged Geysers CA area. Model winds generally agree with observed surface winds, and in some cases may give better estimates of area-averaged flow than point observations. Tracer gas concentration contours agree qualitatively with observed contours, and point predictions of maximum concentrations were correctly predicted to within factors of 2 to 10. Standard statistical tests of model skill showed that the accuracy of the predictions varied significantly from canyon to canyon in the Geysers area. Model wind predictions are also compared to observations from the Savannah River Plant of SC, which

has gently rolling terrain. The model correctly simulated the slower development of drainage winds and slower deepening of the drainage layer in the Savannah River Valley, relative to the Geysers CA simulations. The SC simulations and observations suggest that drainage winds are more frequent in the southeast United States than is generally recognized. They may be responsible for some of the errors in air pollution concentration predictions made by Gaussian models, which assume homogeneous winds and turbulence.

1. INTRODUCTION

Industrialization of the western U.S. has stimulated research on the transport and diffusion of pollutants in regions where the terrain strongly influences low-level winds and turbulence. The Department of Energy (DOE) initiated a research project on flow and diffusion in complex terrain in 1979, called Atmospheric Studies in Complex Terrain (ASCOT). A basic objective of the ASCOT project is improvement in accuracy of surface concentration predictions by drainage flow models.

Drainage winds form whenever there is significant radiative cooling over a sloping surface, although ambient winds may mask their presence to some degree. Meteorologists have been analyzing and modeling the characteristic drainage wind velocity jet for many years, e.g., see one-dimensional analytical models by Prandtl (1942) and Defant (1949, 1951). As a result of the ASCOT project, more complex one-dimensional drainage flow models have been developed and solved numerically by Rao and Snodgrass (1981) and Garrett (1983).

One-dimensional models can only be applied to drainage winds forming over uniform slopes, and so cannot address multi-dimensional effects, such as flow convergence and pooling. Yamada (1981, 1983) and McNider and Pielke (1981) used two and three dimensional simulations to attack the general problem. Three dimensional primitive

equation models produce the most realistic simulations of drainage winds if the grid resolution is fine enough to resolve flows with characteristic depths of 10 to 100 m. Calculations with the necessary space resolution are expensive, so there is a need for models of intermediate complexity which can be applied to practical problems such as industrial site selection.

Several models have been developed since 1970 which could be applied to the drainage flow prediction problem without excessive computational expense. The model by Gutman (1972) solves the equations of motion in a vertical (x-z) plane using idealized eddy viscosity profiles. The equations were scaled for drainage winds, but the surface cooling rate was imposed, and complications such as roughness inhomogeneities were not considered. Gutman claimed qualitative agreement between model predictions and observations but he made no direct comparisons with observations. Danard's (1977) model is a two-dimensional (x,y), time-dependent, primitive equation model in sigma coordinates that adjusts initial wind fields based on measurements of the large scale flow to reflect the effects of field data to test his model, two of which were representative of drainage flow conditions. Scholtz and Brouckaert (1978) developed a two-dimensional (x,y) steady-state vertically-integrated model based on mass and momentum conservation. Each physical process is represented by a flow potential function, which are linearly combined to give the total potential field. The model was designed for stably stratified surface layers, and the

developers used this restriction to link upper geostrophic flow to the surface layer through the pressure gradient, rather than through turbulent momentum transfer. Scholtz and Brouckaert used 76 days of data to test their model, most of which included drainage winds to some degree. The model demonstrated some skill at predicting surface layer winds in complex terrain. Kau et al. (1982) used a statistical approach to wind prediction in complex terrain. The model demonstrates some skill at short-term wind predictions, but it requires site-specific data for determination of coefficients. So it cannot be used for analysis of sites for which there is no meteorological data.

All of the vertically-integrated models described above use arbitrary methods to define the top of the model domain. In contrast, Manins and Sawford (1979a, 1979b) developed and tested a drainage flow model that predicts the depth of the drainage layer by using entrainment theory and laboratory measurements. However, their model treated only the stream-wise space dimension. None of the models included equations for the transport and diffusion of pollutants.

This paper describes a combined dynamical and air pollution model which attempts to correct the deficiencies noted above. The model is specifically designed for drainage flow simulations, which allowed considerable simplification of the governing equations and kept computational demands at a moderate level. In the following

sections, the model is developed and tested with wind and tracer gas data from two areas in a mountainous region and with wind data from a region with gently rolling terrain.

2. DERIVATION OF MODEL EQUATIONS

a. Dynamic Model

The derivation given below is presented in more detail by Garrett and Smith (1982). Dutton (1976) derived the conservation equations for momentum and mass in a generalized coordinate system. Starting with this general system, Pielke and Martin (1981) showed that if a terrain-following vertical coordinate is used, then the criterion

$$\left| \frac{\partial z_g}{\partial x} \right| = \left| \frac{\partial z_g}{\partial y} \right| \ll 1 \quad (1)$$

(where $z_g(x,y)$ is the elevation of the ground above an arbitrary reference level) allows simplification of the general system down to the following set of equations.

$$\frac{\partial \rho u}{\partial x} + \frac{\partial \rho v}{\partial y} + \frac{\partial \rho w}{\partial z} = 0 \quad (2)$$

$$\rho \frac{\partial u}{\partial t} = -\rho u \frac{\partial u}{\partial x} - \rho v \frac{\partial u}{\partial y} - \rho w \frac{\partial u}{\partial z} \quad (3)$$

$$-\frac{\partial p}{\partial x} + \rho f v - \rho g \frac{\partial z_g}{\partial x}$$

$$\rho \frac{\partial v}{\partial t} = -\rho u \frac{\partial v}{\partial x} - \rho v \frac{\partial v}{\partial y} - \rho w \frac{\partial v}{\partial z} \quad (4)$$

$$- \frac{\partial p}{\partial y} - \rho f u - \rho g \frac{\partial z_g}{\partial y}$$

$$\frac{\partial p}{\partial z} = -\rho g \quad (5)$$

There are some differences between Eqs. (2) through (5), and those derived by Pielke and Martin. The transformed vertical coordinate z is defined by

$$z = z_r - z_g \quad (6)$$

where z_r is the vertical coordinate in a rectilinear system.

This transformation is simpler than the one used by Pielke and Martin, which includes a material surface or "lid" at the top of the model domain. The model to be developed here will be a vertically integrated or "slab" model, so a simpler transformation is appropriate. Also, since this model is specifically designed for simulation of drainage winds, which are low-velocity thermally stratified flows, the hydrostatic approximation, Eq. (5), is valid, and Coriolis terms in Eqs. (3) and (4), which involved w were dropped ($w \ll u, v$).

Several steps are next taken to simplify Eqs. (2) through (5) and put them into a form appropriate for drainage flow simulations. First, (3) and (4) are put into the flux form using (2). The Reynolds decomposition into mean and fluctuating components is performed next. After averaging, two simplifying assumptions are

required to obtain closure: 1. triple correlations are negligible and 2. turbulent transport of density fluctuations parallel to the surface is negligible. The velocity components in the drainage layer are treated as if they are constant, and an integration to the top of a variable-depth layer is performed. The Boussinesq approximation is used to replace density fluctuations with potential temperature fluctuations. Next, the assumption that the mesoscale pressure perturbation created by the drainage wind is in hydrostatic balance allows the mesoscale pressure gradient to be expressed in terms of the perturbation potential temperature of the drainage layer and the slope of the drainage layer. Horizontal turbulent transport of momentum is modeled by using the gradient transport hypothesis. The surface stress and the interfacial stress at the top of the drainage layer are modeled with parameterizations similar to those used by Manins and Sawford (1979a). For example,

$$\left. \overline{u'w'} \right|_0 = - C_D U u \quad (7)$$

$$\left. \overline{u'w'} \right|_h = V (u - u_a) E. \quad (8)$$

where C_D is a drag coefficient, and u_a is the x velocity component of the ambient wind above the drainage wind. The velocities U and V are the drainage layer and interfacial shear velocities, respectively, and are defined by

$$U = (u^2 + v^2)^{1/2} \quad (9)$$

$$V = \left[(u - u_a)^2 + (v - v_a)^2 \right]^{1/2}. \quad (10)$$

The variable E is the interfacial entrainment parameter defined by

$$E = A_1 / (S_1 R_i + A_2) \quad (11)$$

where A_1 and A_2 are constants with values of 0.002 and 0.02 respectively, and S_1 is a profile factor with a value of 0.5 (Manins and Sawford, 1979a). The quantity R_i is a layer Richardson number defined by

$$R_i = \frac{-g\theta_D h}{\theta_R U^2} \quad (12)$$

where h is the drainage layer depth, θ_R is a reference potential temperature and θ_D is the perturbation potential temperature of the drainage layer (always negative for drainage winds).

The equations in their final form are

$$\begin{aligned} \frac{\partial u}{\partial t} = & -u \frac{\partial u}{\partial x} - v \frac{\partial u}{\partial y} + K_H \nabla^2 u - \frac{C_D U u}{h} - \frac{V(u - u_a)E}{h} \\ & - f(v_g - v) + \frac{\theta_D g}{\theta_R} \left[\frac{\partial h}{\partial x} + \frac{\partial z_g}{\partial x} \right] \end{aligned} \quad (13)$$

$$\begin{aligned} \frac{\partial v}{\partial t} = & -u \frac{\partial v}{\partial x} - v \frac{\partial v}{\partial y} + K_H \nabla^2 v - \frac{C_D U v}{h} - \frac{V(v - v_a)E}{h} \\ & - f(u - u_g) + \frac{\theta_D}{\theta_R} g \left[\frac{\partial h}{\partial y} + \frac{\partial z_g}{\partial y} \right] \end{aligned} \quad (14)$$

$$\frac{\partial h}{\partial t} = -\frac{\partial uh}{\partial x} - \frac{\partial vh}{\partial y} + K_H \nabla^2 h + VE \quad (15)$$

In Eqs. (13) through (15) K_H is the horizontal eddy viscosity, which is defined in terms of the horizontal wind shear (see Smagorinsky et al., 1965 and Anthes and Warner, 1978). In (15), the term VE represents turbulent entrainment into the drainage layer normalized by the mean density, i.e.,

$$VE = - \frac{\overline{\rho'w'}|_h}{\bar{\rho}} \quad (16)$$

Note that the mesoscale pressure perturbation terms in (13) and (14) which involve gradients of h , are independent of the local slope gradient. These are the terms responsible for forcing flow in the valley floor which has little or no local tilt. These terms are also responsible for deceleration of downslope flows into a pool of cold air.

If Θ_D and the geostrophic and ambient velocity components are prescribed, then Eqs. (13) through (15) are a closed system that can be solved numerically. The geostrophic and ambient velocity components can be determined from measurements or set equal to zero for a simulation of pure drainage winds. A space and time dependent specification for Θ_D would require an additional prognostic equation. But observations of drainage winds show that they form rapidly after radiation sunset and remain fairly steady through the night, unless they are disturbed by a synoptic-scale event. Data volumes compiled by (Gudiksen, 1981) contain surface data with excellent examples of steady drainage winds. This implies that Θ_D can be treated as a constant as a first approximation. Numerical

simulations (Garrett, 1983) and ASCOT tethered sonde data (Cudiksen, 1981) both suggest that the magnitude of Θ_D averaged over the depth of the drainage layer is about -1°C . This value was used in the simulations described in Section 4 of this report.

b. Transport and Diffusion Model

A simple Monte Carlo (MC) model described by Hanna et al. (1982) was chosen to perform transport and diffusion simulations. This model is attractive because it is mathematically simple but flexible. Monte Carlo models are also free from numerical stability and error problems and the scale-dependent diffusion problem associated with the solution of an advection-diffusion equation describing the conservation of a gaseous pollutant.

In this MC model, each velocity component is divided into mean and turbulent components, i.e., $u = \bar{u} + u'$. The mean component is provided at each time step by Eqs. (13) and (14). The behavior of the turbulent component is governed by

$$u'(t + dt) = u'(t)R(dt) + u''(t + dt) \quad (17)$$

where t is time, dt is the time step, R is the autocorrelation coefficient, and u'' is a random component. The random component is defined by

$$u'' = \pm(-2\sigma_{u''}^2 \ln \xi)^{1/2} \quad (18)$$

where $\sigma_{u''}^2$ is the variance of the random components and ξ is a random number constrained by $0 < \xi < 1$. The sign of u'' is also randomly selected. Eq. (18) generates a frequency distribution of u'' similar to a normal distribution but skewed toward larger values

of u'' . This characteristic should improve the model performance because Hanna (1981b) found that drainage winds are very turbulent for such stable, weak flows.

The random component is related to the turbulent component by

$$\sigma_{u''}^2 = \sigma_{u'}^2 (1 - R^2(dt)) \quad (19)$$

which is required to conserve kinetic energy. The autocorrelation function $R(dt)$ is defined by

$$R(dt) = \exp(-dt/T_L) \quad (20)$$

where T_L is the Lagrangian time scale.

Determining the best way to estimate T_L for drainage winds proved to be a problem. Hanna (1981a) described a method in which T_{EP} , the time period of peak energy in the Eulerian turbulent energy spectrum, is related to T_L . Hanna showed that the Eulerian time scale T_E can be approximated by $T_E = T_{EP}/6$. Following Corrsin (1963), Hanna related T_E to T_L with

$$T_L = \frac{0.6 T_E U}{\sigma_v} \quad (21)$$

where σ_v is the standard deviation of the velocity fluctuations, which is assumed to equal $\sigma_{u'}$. Binkowski (1978) found that σ_v can be related to the friction velocity u_* by $\sigma_v = 1.78 u_*$ in neutral conditions. Hanna (1981b) showed that turbulence in drainage winds near Geysers, CA was representative of neutral stability (Pasquill D) even though the flow is stably stratified.

If u_* is related to U by

$$u_*^2 = C_D U^2 \quad (22)$$

where C_D is a drag coefficient appropriate for a forested area, then T_L can be computed, given a value of T_{EP} . Murphy et al. (1977) found that C_D was 0.02 for a southern pine forest, so C_D should be about 0.01 for a partially forested area such as Geysers, CA. Doran and Horst (1981) analyzed ASCOT data from the Geysers area and found that $T_{EP} \approx 90$ min. They suggested that this low frequency peak was the result of oscillations inherent to drainage winds. If T_{EP} is 90 min, then Eq. (21) gives a T_L of about 45 min, which is very large. Hanna's (1981a) relationship between T_E and T_{EP} was derived from an analysis of daytime convective boundary layer turbulence data, so its use here is a tentative step toward wider application of the relationship.

Using a more straightforward empirical approach, Fosberg et al. (1982) computed T_L from data on the dispersion of tetroon clusters released into drainage winds in the Geysers area. They repeatedly found T_L to be about 5 min, which is much closer to the typical magnitude of T_L . However, the much larger values of T_L derived from the analysis by Doran and Horst (1981) may be more physically significant if turbulent diffusion in drainage winds is largely brought about by low frequency, large scale sloshings. A T_L representative of these large oscillations probably would be fairly uniform over the area affected by the drainage wind. Since the

buoyancy deficit is treated as a constant in Eqs. (13) and (14), the model winds tend to become steady after an hour or two of integration. Selection of a T_L representative of the mesoscale variability of the flow compensates for the simplified approach to modeling the buoyancy force. In Section 4, Monte Carlo diffusion simulations with small and large values of T_L are compared.

3. NUMERICAL METHODS

The system of dynamical equations was solved numerically with a second-order finite difference scheme. Advection of mass and momentum was calculated by the second upwind differencing or "donor cell" method, Roache (1976), Gentry et al. (1966). In early tests of the model, the more accurate but more computationally expensive fourth order differencing scheme by Crowley (1968) was compared to solutions from the second order scheme. There was very little difference, so the second order scheme was used. The computations were found to be stable when the time step satisfied the condition

$$\Delta t < 1 / \left(\frac{|u|}{\Delta x} + \frac{|v|}{\Delta y} \right) .$$

Calculation time steps were based on this criterion and the assumption that velocity components would not exceed 5.0 m/s in magnitude. Simulations of up to 1440 time steps were run and no stability problems were encountered.

Initial conditions for the integration assumed a drainage layer depth of 10 m. The initial velocity components were set equal to ambient wind values or zero. Boundary values at points of flow into the computational domain were fixed at the initial values. Open

boundary conditions for the wind components and drainage layer depth were used at points of outflow from the grid. A minimum drainage depth was set at 5.0 m to simulate continuous radiational cooling at the ground.

Topography gradients were calculated at each grid by averaging the change in elevation around the point. For example

$$\frac{\partial z}{\partial x} \Big|_{i,j} = \frac{1}{2} \left[\frac{z_{i+1/2,j-1/2} - z_{i-1/2,j-1/2}}{\Delta x} + \frac{z_{i+1/2,j+1/2} - z_{i-1/2,j+1/2}}{\Delta x} \right]$$

Model simulations were run over three separate topography grids. For the Anderson Creek region of the Geyser's area, a 29 x 29 grid with $\Delta x = \Delta y = 250$ m was used. A time step of 20 s was employed in the Anderson Creek simulations. For the Big Sulfur Creek region of the Geyser's area, a 51 x 41 grid was used with $\Delta x = \Delta y = 225$ m. A 20 s time step was again used. In the Savannah River Plant simulations, a 45 x 60 grid was used with $\Delta x = \Delta y = 2000$ m. A conservative time step of 60 s was employed for these calculations.

The simple Monte Carlo technique described by Hanna et al. (1982) was used to calculate tracer concentration profiles. The Lagrangian calculation method offered the major advantage of exactly conserving the amount of tracer material. The computations followed 6000 particles using a time step of 60 s. To some extent, the short timestep desensitized the model response to variations in the magnitude of T_L (see discussion in previous section). The mean wind field was obtained from the solution to the dynamical equations and updated every 5 min. That is, the Monte Carlo simulation was run for 5 time steps during which the mean wind field was

assumed to remain constant. The dynamical calculation was then continued to simulate the next 5-min interval and the process repeated. Consistent with the second order finite differencing, velocity components at each particle position were determined by two-dimensional linear interpolation from the grid points. To model tracer release experiments, the particles were assumed to be released at a constant rate during the first part of the Monte Carlo simulation. The total release time corresponded to that of the field experiments. Model predicted concentrations could be reported as instantaneous values at specified times or the values integrated over some period of time using a trapezoidal rule. The integrated results were used to simulate the experimental sampling technique employed to obtain the Geysers' area field data. Instantaneous tracer concentrations at a grid point were calculated by summing all particles within $\pm\Delta x/2$ and $\pm\Delta y/2$ of the point and dividing by the volume. The volume at a grid point was calculated as the drainage depth multiplied by $\Delta x\Delta y$.

4. SIMULATIONS COMPARED TO OBSERVATIONS

a. California Geysers Area

Simulations were performed for two areas in the Geysers region of northern California, where detailed measurements of drainage winds and tracer gas dispersion are available (Gudiksen, 1981). This is a region of rugged terrain, where slopes of 10° to 15° are common, and 20° slopes are found in some places. A 20° slope probably comes close to violating the constraint given in Eq. (1).

However, the errors caused by the steep slopes probably were no larger than those caused by vertical integration and a constant buoyancy deficit. Figs. 1 and 2 show the topography of the Anderson Creek and Big Sulfur Creek areas. The model was also tested with the gentler terrain in the vicinity of the Savannah River Plant (SRP) in South Carolina. The terrain slopes in the SRP area are on the order of 1° .

The Geysers area simulations were conducted on rectangular grids 7 to 11 km on a side with mesh sizes of 225 to 250 m (see Section 3). Simulations with and without geostrophic and ambient winds were performed, but only those simulations in which the geostrophic and ambient winds were set to zero will be discussed here, because addition of the ambient winds and pressure gradients did not improve model performance. See Garrett and Smith (1982) for details on simulations that included ambient winds. This suggests that drainage winds forming in deep canyons are decoupled from the synoptic scale flow. Scholtz and Brouckaert (1978) observed this decoupling in their study of drainage winds in South Africa. However, drainage winds that form on more exposed slopes are not decoupled and interact strongly with the ambient winds (Garrett, 1983).

Fig. 3 shows model predictions of the simulated wind field for Anderson Creek 6 hr after starting from an atmosphere at rest. A full feather on a vector represents 1 m/s and a half feather represents 0.5 m/s. The simulation reached a steady-state solution

quickly; the wind field was almost identical after 1 hr of simulated time. This behavior conforms to observations of well-developed drainage winds and agrees with the analysis of Gutman (1972) which predicts a development time for drainage winds on the order of 10 min.

Fig. 4 shows the predicted drainage flow depths in meters and corresponds to the winds in Fig. 3. The depths increased rapidly during the first hour of simulated time, like the winds. But there was some increase in depth in the main pooling area after the first hour, as the flow off the slopes converged on the lower part of Anderson Creek Valley. The maximum depths in Fig. 4 of around 250 m are in general agreement with observed drainage flow depths, based on tracer gas diffusion (Gudiksen, 1981).

In Fig. 5 observed winds are compared to predicted winds at the National Center for Atmospheric Research (NCAR) Portable Automated Mesonet (PAM) surface stations. The observed wind vectors in Fig. 5 are averages of 4 hr of observations (1000 to 1400 GMT on 20 September 1980) taken at 4 m above the ground. There is generally good agreement with a few exceptions, mostly on the ridges. In two cases the simulated wind vectors appear to be in better agreement with the general terrain and flow than the observed vectors. Small scale topographic features, such as hillocks or ravines, may have caused those anomalies. The average observed wind speed from the PAM stations was 1.30 m/s, compared to the averaged computed value from the same locations of 1.46 m/s.

Model predictions of perfluorocarbon (PDCH) concentrations in ppt were compared to observations taken on the night of 19-20 September 1980. Since all of the experimental data (Gudiksen, 1981) was reported in ppt, this unit of measurement has been used for convenience. The reported concentrations in ppt may be converted into $\mu\text{g}/\text{m}^3$ by multiplying by a factor of 0.0178. Figs. 6a, 6b, and 6c show observed and computed PDCH concentrations averaged over a 2-hr sampling period, starting at the beginning of the 1 hr release. The observed contours were drawn subjectively by the ASCOT scientists who made the measurements. Fig. 6b presents predicted contours based on a Lagrangian time scale (T_L) of 45 min, and 6c presents results for a 5-min T_L . It is difficult to say which T_L produced the best agreement, because both simulated distributions have good and bad features. In Fig. 6b the plume is too wide, but the bulge in the contours at the outflow of Putah Creek is reproduced, whereas in Fig. 6c it is not. But the width of the plume in Fig. 6c is closer to the observed width. Neither of the simulations predicted the high concentrations (greater than 1000 ppt) in Gunning Creek just down from the release point. Possibly, these high concentrations were caused by trapping of the PDCH by the forest along the creek bed.

Time series of PDCH concentrations were available at Station S-3 (Fig. 1). Fig. 7 compares the simulated and observed time series. The maximum observed concentration is predicted fairly

well, to within a factor of three. The simulated PDCH plume precedes the observed plume, possibly because the actual plume tilted downwind with height due to vertical wind shear. Surface stations would miss the elevated leading edge, whereas the simulated plume arrives at the same time at all heights, because the model equations are vertically integrated.

Another perfluorocarbon, PMCH ($\mu\text{g}/\text{m}^3 = 0.0156 \times \text{ppt}$), was released from the upper end of Anderson Creek on the night of 19-20 September 1980. The general concentration contours are correctly duplicated by the model for the first 2 hr of the release (Figs. 8a and 8b). The longer T_L of 45 min was used in this simulation. After 6 hr of simulated time the model correctly predicted that almost all of the PMCH exited the lower end of Anderson Creek (concentrations 1 ppt or less). The simulated and observed PMCH time series at Station S-4 are compared in Fig. 9. As with the PDCH release, the simulated plume arrived early and did not leave behind a tail of low concentration. The maximum concentration was underpredicted by about a factor of 10, and the general under-prediction by the model for the PMCH release suggests that much of the simulated plume missed S-4, traveling south of it (see Figs. 1 and 8).

The geometry of Big Sulfur Creek (Fig. 2) is simpler than the Anderson Creek geometry, so the model simulations were more accurate. After 2 hr of simulated time the model predicted a confined, uniform drainage flow. Very little wind data was taken in Big

Sulfur Creek during the PDCH release, so model skill will be assessed only from the tracer measurements and simulations ($T_L = 45$ min). Simulated and observed 1 hr average concentration contours (Figs. 10a, b) for the second hour of the release are in good qualitative agreement, as was the case for the other hours of the release. The simulated and observed time series at Stations S-2 and S-3 (Figs. 11 and 12) are generally in better agreement than the Anderson Creek time series. Although the maximum at S-2 was underpredicted by a factor of 3, the timing of the arrival and the concentration tail were more faithfully reproduced than they were at the Anderson Creek stations. The simulated time series at S-3 also shows some improvement, with an excellent prediction of the maximum concentration and an appreciable concentration tail.

To summarize, the Geysers area simulations showed that the model described in Section 2 can predict maximum pollutant concentrations within drainage winds to within factors of 2 to 10 at a given point. There is qualitative agreement between concentrations contours, and the Monte Carlo diffusion model does not appear to be sensitive to the value of T_L used.

b. Savannah River Plant

The SRP is located in central South Carolina and is bounded in the south by the Savannah River, which separates Georgia from South Carolina. A network of meteorological towers provide each production area with wind and turbulence information (Fig. 13). At A, F, H, G, K, and P Areas there are 61 m towers and at D Area there is

a 61 m tower (D-2) and a 10 m (D-1) tower. The D Area towers are the only ones in the Savannah River Valley (SRV). At the site marked T there is a 300 m television tower which has instruments at 7 levels, ranging from 2 to 300 m. Garrett, Buckner, and Mueller (1983) describe the SRP meteorological data acquisition system in more detail.

The SRP drainage flow simulations were performed on a 90 x 120 km grid with a 2 km mesh. The large grid and coarse mesh were needed to ensure that a sufficiently large part of the Savannah River Valley was covered for organized flow to develop. The largest slopes in the grid were in the grid cells covering the transition from the SRV to the gently rolling uplands beyond. These slope angles were about 1° . The predicted rate of development of drainage flow over the SRP area was much slower than in the Geysers area. Fig. 14 shows a sequence of vector fields representing the predicted flow after 2, 4, and 8 hr of simulated time, starting from an atmosphere at rest. After 2 hr, the only organized flow was a strip of katabatic winds flowing into the SRV from the northeast. After 4 hr there was sufficient pooling for organized flow down the SRV to begin. After 8 hr the flow volume down the SRV had increased significantly, but the simulation had finally reached a near steady-state. After 8 hr the maximum wind speeds were only 1 to 1.5 m/s, weaker than the 2 to 2.5 m/s winds observed and predicted for the Geysers area. The drainage flow

depths for the SRP area also increased slowly over the 8 hr simulation, reaching a maximum depth of 70 m in the SRV, with 10 to 40 m depths elsewhere.

Hourly average wind vectors from SRP (Fig. 15) show the slow development of drainage winds in the SRV. The data represent the 61 m level at all areas, plus the 10 m level at D Area. This series is not unusual, because polar highs centered over the southeast United States during the fall and winter frequently produce the dry conditions with light winds required for drainage flow development. The C-Area tower was out of operation.

Fig. 15a shows well-mixed conditions with uniform flow late in the afternoon (2230 GMT) on January 27, 1982. A surface temperature inversion formed quickly after radiation sunset, but the wind vectors showed no indication of drainage winds until local midnight (Fig. 15b), when the D1 (10 m) tower appeared to be in katabatic winds flowing toward the river basin. By 0730 GMT (Fig. 15c) the D1 tower winds indicated a shift from katabatic flow to organized drainage flow down the SRV. At sunrise (Fig. 15d) the flow had deepened enough to control the winds on the 61 m (D2) tower. In agreement with model simulations, none of the other towers appeared to be within the drainage layer.

The frequent appearance of shallow drainage winds at the SRP is of great practical significance, because many power plants and other industrial sites in the southeast United States are in rolling terrain. If drainage winds are as frequent at these sites

as they are at the SRP, then there will be many nights when meteorological measurements at stack level will not be representative of low-level flow in the area, including the air just below the instrumentation level. Transport and diffusion predictions in these conditions may be grossly in error, particularly if pollutants are released into the drainage layer, and winds are measured above it. This problem is made more noteworthy by the fact that pollutant concentrations remain high in drainage flows, due to their shallowness and limited vertical diffusion. Also, drainage winds tend to seek populated areas, because they flow downhill toward valleys and plains.

5. STATISTICAL ANALYSIS OF MODEL SKILL

The discussion in Section 4a suggests that the model described in Section 2 has some ability to predict pollutant concentrations within drainage winds. Quantitative methods for evaluating model skill are receiving more attention, e.g., see Fox (1981) and Weber et al. (1982). In this section, simple statistical measures of correlation, bias and dispersion are used to quantify the model performance. The results are tabulated in Tables 1-4. Two experiments from the data compiled by Gudiksen (1981) were selected, the nights of 15-16 September (Experiment 2) and 19-20 September (Experiment 4). Both nights had well-defined drainage winds.

Tables 1 and 2 show results for the PDCH and PMCH tracer releases into the Anderson Creek valley. The tables are self-explanatory, except for the phrase "% within Factor of 5" which

refers to the ratio of predicted to observed concentrations. The means, root-mean-square (RMS) errors, standard deviations and biases are in parts per trillion (ppt). Statistics were calculated for 0 to 2 and 2 to 4 hr after the start of traces gas emissions. The skill tests indicate that the PDCH simulation was poorer than the PMCH simulation. For example, none of the correlation coefficients in Table 1 are significant at the 5% level, whereas all four correlation coefficients in Table 2 are significant. More of the predictions were correct to within a factor of 5 in the PMCH simulation. In contrast, subjective evaluation of Figs. 6, 7, 8, and 9 suggests about equal skill. Part of the poorer statistical performance of the model with the PDCH tracer data was probably caused by the small area of high concentrations (>1000 ppt) that was not predicted by the model. Some of the error in the PDCH and PMCH simulations can be attributed to the lack of spatial averaging in the observed data. The lack of averaging is most apparent in the observed standard deviations, which are much larger than the predicted standard deviations. The stations were too sparse and unevenly spaced to allow averaging over areas corresponding to the model grid volumes. This is a common problem that can only be corrected by large expenditures for comprehensive data sets designed for model validation.

The meaning of the results in Tables 1 and 2 becomes clearer when they are compared to Table 3. In Table 3, the PDCH and PMCH observations from Experiment 2 are compared to the observations

from Experiment 4. In other words, the observations in Experiment 2 were used as predictions, and were compared to the observations in Experiment 4. The correlation coefficients are higher than they were for the model predictions, and more of the ratios of predictions to observations are within a factor of 5, relative to the corresponding ratios in Tables 1 and 2. But the RMS error and bias results in Table 2 are similar to those in Table 3. If the night-to-night variability in drainage winds is a measure of the inherent uncertainty of these flows, then there is room for model improvement, unless the discrepancy is largely due to the lack of spatial averaging of the observations.

The results in Table 4 for Big Sulfur Creek are better, verifying the subjective impression in Section 3. Part of the improvement may simply be due to more even spacing of stations in Big Sulfur Creek, relative to Anderson Creek. Part of it may also be due to the simpler terrain. Several creek valleys contribute to the Anderson Creek drainage winds, whereas Big Sulfur Creek is isolated. The average predicted concentrations were usually lower than the average observed concentrations from the Big Sulfur Creek simulations, as they were in the Anderson Creek simulations. This is probably a result of the vertical integration of the model equations, because concentrations from surface releases in drainage winds will tend to decrease with height. A vertical distribution function might help correct this bias.

TABLE 1**Anderson Creek PDCH Experiments Compared With Model Predictions**

	Exp. #2 (0-2 hr)	Exp. #2 (2-4 hr)	Exp. #4 (0-2 hr)	Exp. #4 (2-4 hr)
No. Data Points	37	35	39	34
RMS Error	254.0	19.7	332.9	20.9
Mean Prediction	12.6	0.39	13.3	0.82
Standard Deviation	461.8	0.60	488.4	4.70
Mean Observation	51.8	5.90	63.7	8.62
Standard Deviation	65690.0	367.3	112510.0	406.3
Correlation Coeff.	0.13	0.00	0.13	0.26
Regression Slope	0.01	0.00	0.01	0.03
Model Bias	39.2	5.51	50.4	7.80
% Within Factor of 5	16.7	17.9	39.5	24.0

TABLE 2**Anderson Creek PMCH Experiments Compared With Model Predictions**

	Exp. #2 (0-2 hr)	Exp. #2 (2-4 hr)	Exp. #4 (0-2 hr)	Exp. #4 (2-4 hr)
No. Data Points	38	36	39	38
RMS Error	142.8	2.52	64.0	3.63
Mean Prediction	12.3	0.40	10.9	0.67
Standard Deviation	428.8	0.80	297.8	4.65
Mean Observation	47.0	1.08	26.5	1.80
Standard Deviation	24550.0	7.11	5657.0	12.9
Correlation Coeff.	0.81	0.40	0.77	0.34
Regression Slope	0.11	0.13	0.18	0.20
Model Bias	34.7	0.69	15.6	1.12
% Within Factor of 5	26.7	34.8	36.1	25.8

TABLE 3**Anderson Creek Experiment #2 Compared With Experiment #4**

	PDCH (0-2 hr)	PDCH (2-4 hr)	PMCH (0-2 hr)	PMCH (2-4 hr)
No. Data Points	33	34	35	34
RMS Error	99.5	3.29	96.8	1.61
Mean Observation for #2	58.1	6.07	51.0	1.15
Standard Deviation	73520.0	377.4	26510.0	7.47
Mean Observation for #4	73.6	7.21	28.2	1.79
Standard Deviation	132900.0	377.3	6277.0	13.7
Correlation Coeff.	0.99	0.99	0.92	0.94
Regression Slope	0.74	0.99	1.89	0.69
Model Bias	15.6	1.15	-22.8	0.64
% Within Factor of 5	29.6	64.5	67.6	76.5

TABLE 4**Big Sulfur Creek PDCH Experiments Compared with Model Predictions**

	Exp. #1 (0-1 hr)	Exp. #1 (1-2 hr)	Exp. #1 (2-3 hr)	Exp. #1 (3-4 hr)
No. Data Points	29	41	40	38
RMS Error	41.8	14.8	2.51	1.20
Mean Prediction	15.0	9.9	3.23	0.58
Standard Deviation	880.0	130.5	5.87	0.45
Mean Observation	29.8	14.4	2.10	0.82
Standard Deviation	3909.0	472.1	5.92	2.45
Correlation Coeff.	0.85	0.80	0.57	0.71
Regression Slope	0.41	0.42	0.56	0.30
Model Bias	14.8	4.5	-1.13	0.24
% Within Factor of 5	48.0	55.3	78.4	80.0

6. CONCLUSIONS

The drainage flow model described in this paper has the following features which make it attractive as a practical tool for estimating the concentrations of pollutants released into nocturnal drainage winds.

1. No wind or temperature data is needed to start the model. A surface drag coefficient and Eulerian or Lagrangian time scale are required, but the model is not sensitive to their exact value. High resolution topographic data is required.
2. The model has been tested successfully at sites with rugged mountainous terrain and at a site with gently rolling terrain.
3. The model is two-dimensional (vertically integrated) so its computational requirements are moderate.
4. Maximum pollutant concentrations were predicted to within factors of 2 to 5 at specific points, based on observed and simulated concentration time series.
5. Simulated concentration contours were qualitatively correct and plume transport speeds were correctly predicted.
6. Objective, quantitative tests of model skill produced mixed results, with a good performance in Big Sulfur Creek, but not as good in Anderson Creek. The results probably would have been better if the stations had been dense enough to allow spatial averaging of the observations corresponding to the model grid resolution.

ACKNOWLEDGMENTS

We gratefully acknowledge the stimulating discussions that we had with the other scientists participating in the U.S. Department of Energy's ASCOT project. The model validation would not have been possible without the excellent field data gathered by ASCOT scientists in the Geysers, CA area, and by technical support groups at the Savannah River Plant. This paper was prepared in connection with work done under Contract No. DE-AC09-76SR00001 with the Department of Energy.

REFERENCES

- Anthes, R. A., and T. T. Warner, 1978: Development of Hydrodynamic Models Suitable for Air Pollution and Other Mesometeorological Studies. Mon. Wea. Rev., 106, 1045-1078.
- Binkowski, F. S., 1978: A Simple Semi-Empirical Theory for Turbulence in the Atmospheric Surface Layer. Atmos. Environ., 13, 247-253.
- Corrsin, S., 1963: Estimation of the Relation Between Eulerian and Lagrangian Scales in Large Reynold's Number Turbulence. J. Atmos. Sci., 20, 115-119.
- Crowley, W. P., 1968: Numerical Advection Experiments. Mon. Wea. Rev., 96, 1-11.
- Danard, M., 1977: A Simple Model for Mesoscale Effects of Topography on Surface Winds. Mon. Wea. Rev., 105, 572-581.
- Defant, F., 1949: Zur Theorie der Hangwinde, nebst Bemerkungen zur Theorie der Berg- und Talwinde, Arch. Meteor. Geophys. Bioklin. A1, 421-450.
- Defant, F., 1951: Local Winds. Compendium of Meteorology. T. F. Malone, ed., Amer. Meteor. Soc., 655-672.
- Doran, J. C., and T. W. Horst, 1981: Velocity and Temperature Oscillations in Drainage Winds. J. Appl. Meteor., 20, 361-364.
- Dutton, J. A., 1976: The Ceaseless Wind, An Introduction to the Theory of Atmospheric Motion. McGraw-Hill, 579 pp.

- Fosberg, M. A., L. M. Lanham, and B. A. Taylor, 1982: Characterization of the Transport and Diffusion Processes in the Geysers Geothermal Area of California. Rep. #DE-AP-03-80-9F-11331, 10 pp. [Available from USDA Forest Service Forest Fire Laboratory, Riverside, CA].
- Fox, D. G., 1981: Judging Air Quality Model Performance - Review of the Woods Hole Workshop. Preprints, Fifth Symp. on Turbulence, Diffusion, and Air Pollution, Atlanta, Amer. Meteor. Soc., 14-16.
- Garrett, A. J., and F. G. Smith, 1982: A Two-Dimensional Dynamical Drainage Flow Model with Monte Carlo Transport and Diffusion Calculations. DP-1639, 67 pp. [Available from E. I. du Pont de Nemours & Co., Savannah River Laboratory, Aiken, SC 29808.]
- Garrett, A. J., 1983: Drainage Flow Prediction with a One-Dimensional Model Including Canopy, Soil, and Radiation Parameterizations. J. Climate and Appl. Meteor., 22, 79-91.
- Garrett, A. J., M. R. Buckner, and R. A. Mueller, 1983: The Weather Information and Display Emergency Response System. Nucl. Tech., 60, 50-59.
- Gentry, R. A., R. E. Martin, and B. J. Daly, 1966. An Eulerian Differencing Method for Unsteady Compressible Flow Problems. J. Computational Physics, 1, 87-118.

- Cudiksen, P. H., 1981: ASCOT Data from the 1980 Field-Measurement Program in Anderson Creek Valley, California. [Available from Lawrence Livermore National Laboratory, Livermore, CA.]
- Gutman, L. N., 1972: Introduction to the Non-linear Theory of Mesoscale Meteorological Processes, TT 71-50132 (translation), Israel Program for Sci. Translations, Jerusalem, 224 pp. [Available from NTIS, Springfield, VA 22161.]
- Hanna, S. R., 1981a: Lagrangian and Eulerian Time Scale Relations in the Daytime Boundary Layer. J. Appl. Meteor., 20, 242-249.
- Hanna, S. R., 1981b: Diurnal Variations of Horizontal Wind Direction Fluctuations in Complex Terrain at Geysers, CA, Boundary Layer Meteor., 21, 207-213.
- Hanna, S. R., G. A. Briggs, and R. P. Hosker, 1982: Handbook on Atmospheric Diffusion. DOE/TIC-11223, 102 pp. [Available from Office of Health and Environmental Research, Dept. of Energy, NTIS DE81009809].
- Kau, W. S., H. N. Lee, and S. K. Kao, 1982: A Statistical Model for Wind Prediction at a Mountain and Valley Station Near Anderson Creek, California. J. Appl. Meteor., 21, 18-21.
- Manins, P. C., and B. L. Sawford, 1979a: A Model of Katabatic Winds, J. Atmos. Sci., 36, 619-630.
- Manins, P. C., and B. L. Sawford, 1979b: Katabatic Winds: A Field Case Study. Quart. J. Roy. Met. Soc., 105, 1011-1025.

- McNider, R. T. and R. A. Pielke, 1981: Diurnal Boundary Layer Development Over Sloping Terrain. J. Atmos. Sci., 38, 2198-2212.
- Murphy, C. E., T. R. Sinclair, and D. R. Knoerr, 1977: An Assessment of the Use of Forests as Sinks for the Removal of Atmospheric Sulfur Dioxide. J. Env. Quality, 6, 338.
- Pielke, R. A. and C. L. Martin, 1981: The Derivation of a Terrain-Following Coordinate System for Use in a Hydrostatic Model. J. Atmos. Sci., 38, 1707-1713.
- Prandtl, L., 1942: *Führer durch die Stromungslehre*, Vieweg u. Sohn. Braunschweig. [Available in English as *Essentials of Fluid Dynamics*, Hafner Publishing Co., New York, 1952, 452 pp., 373-375.]
- Rao, K. S. and H. F. Snodgrass, 1981: A Nonstationary Nocturnal Drainage Flow Model. Bound. Layer Meteor., 20, 309-320.
- Roache, P. J., 1976: Computational Fluid Dynamics, Hermosa Pub., Albuquerque, NM, 446 pp.
- Scholtz, M. T., and C. J. Brouckaert, 1978: Modeling of Stable Air Flow Over a Complex Region. J. Appl. Meteor., 17, 1249-1257.
- Smagorinsky, J., S. Manabe, and J. L. Holloway, Jr., 1965: Numerical Results from a Nine-Level General Circulation Model of the Atmosphere. Mon. Wea. Rev., 93, 727-768.
- Weber, A. H., M. R. Buckner, and J. H. Weber, 1982: Statistical Performance of Several Mesoscale Atmospheric Dispersion Models. J. Appl. Meteor., 21, 1633-1644.

Yamada, T., 1981: A Numerical Simulation of Nocturnal Drainage

Flow, J. Meteor. Soc. Japan, 59, 108-122.

Yamada, T., 1983: Simulations of Nocturnal Drainage Flows by a

q^2L Turbulence Closure Model. J. Atmos. Sci., 40, 91-106.

FIGURE LEGENDS

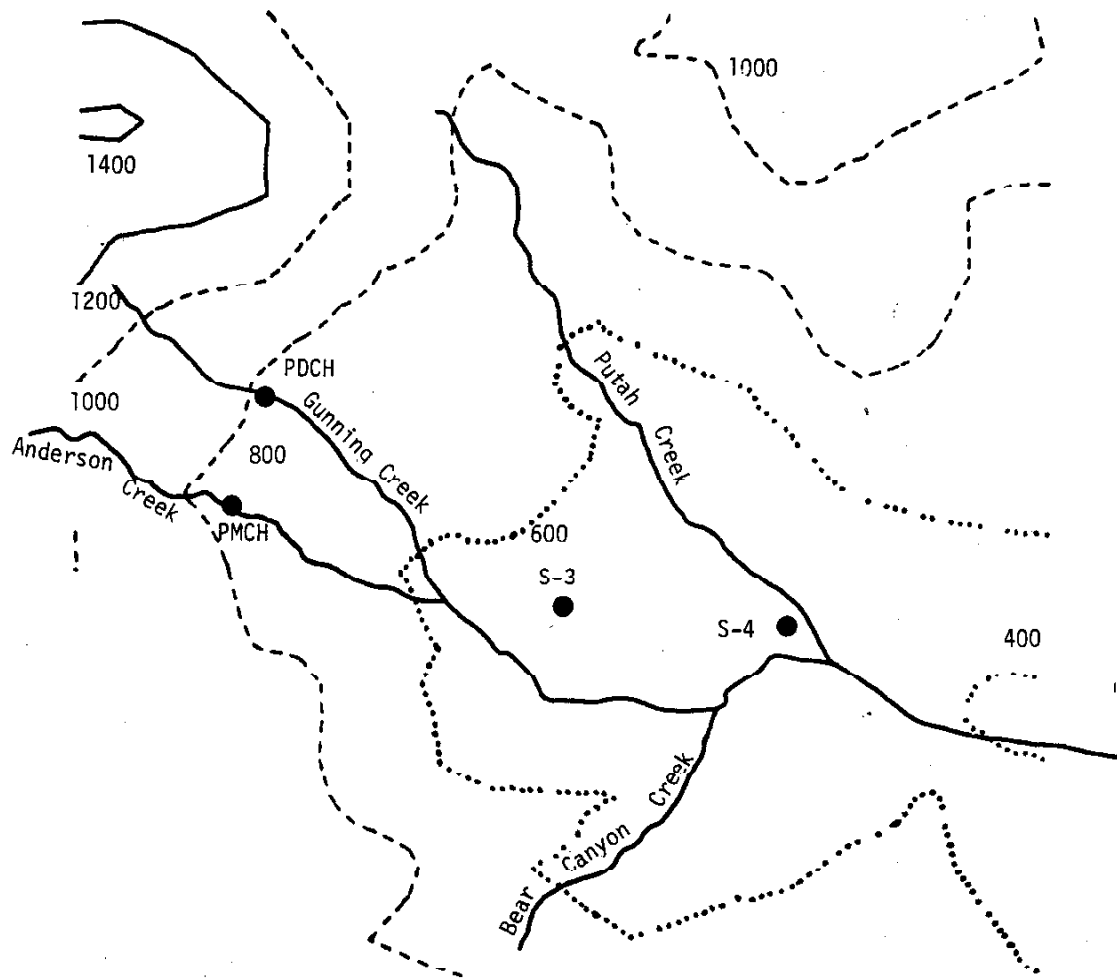
- Fig. 1 Anderson Creek area computational domain (7 km by 7 km) and topography, with topography contours in meters and perfluorocarbon tracer release sites and receptor locations for time series measurements. The more numerous time-integrated sampler sites are not shown.
- Fig. 2 As in Fig. 1, but for Big Sulfur Creek area of Geysers, CA region.
- Fig. 3 Simulated wind field for Anderson Creek area 6 hr after starting from an atmosphere at rest. A full feather on a vector represents 1 m/s and a half feather is 0.5 m/s.
- Fig. 4 Predicted drainage flow depths in meters for Anderson Creek after 6 hr of simulated time. Topographic height contours in meters are plotted outside the computational domain.
- Fig. 5 Observed and predicted wind vectors at NCAR PAM stations for Anderson Creek area. Solid vectors are observed; dashed are simulated. A full feather is 1 m/s; one half feather is 0.5 m/s. Observed wind vectors are averages of 4 hr of observations (1000 to 1400 GMT on 20 September 1980).
- Fig. 6 Observed (6a) and predicted (6b,c) perfluorocarbon (PDCH) concentrations in ppt averaged over a 2-hr sampling period for Anderson Creek area. Fig. 6b gives results for a Lagrangian time scale (T_L) of 45 min, and 6c shows results for a T_L of 5 min. See Fig. 1 for release point.

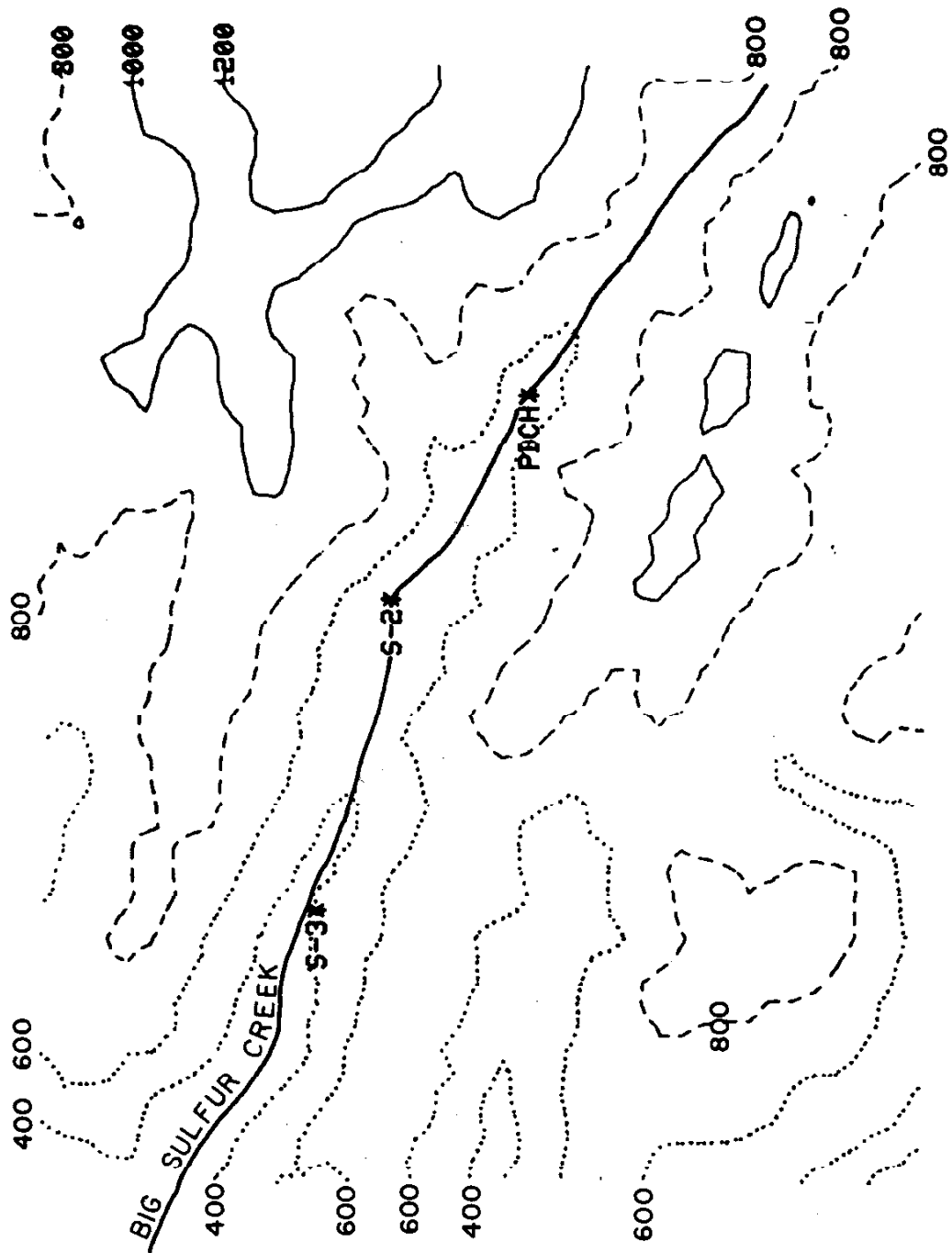
FIGURE LEGENDS (Contd)

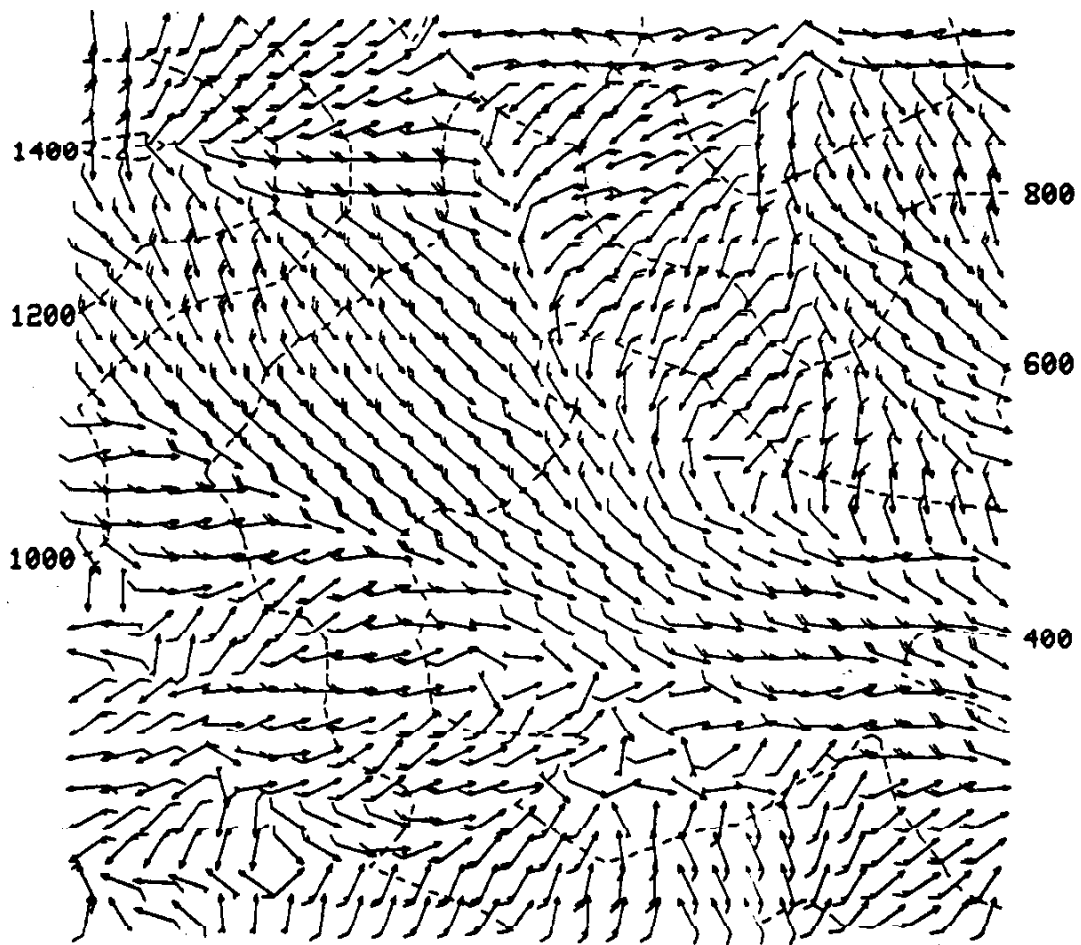
- Fig. 7 Time series of predicted (dashed) and observed (solid) PDCH concentrations in ppt for station S-3 in the Anderson Creek area (see Fig. 1). Observed and computed concentrations are 15 min averages.
- Fig. 8 Observed (8a) and predicted (8b) perfluorocarbon (PMCH) concentrations in ppt averaged over a 2-hr sampling period for Anderson Creek area. T_L was 45 min. See Fig. 1 for release point.
- Fig. 9 As in Fig. 7, but for PMCH concentrations at station S-4 (see Fig. 1).
- Fig. 10 Predicted (12a) and observed (12b) one-hour average PDCH concentrations in ppt for Big Sulfur Creek area for second hour of release.
- Fig. 11 Predicted (dashed) and observed (solid) time series of PDCH concentrations in ppt for station S-2 in Big Sulfur Creek area.
- Fig. 12 As in Fig. 13, but for station S-3.
- Fig. 13 Locations of Savannah River Plant 61 m meteorological towers (A, F, H, C, K, P, and D), 300 m instrumented television tower (T), and local streams flowing into the Savannah River.

FIGURE LEGENDS (Contd)

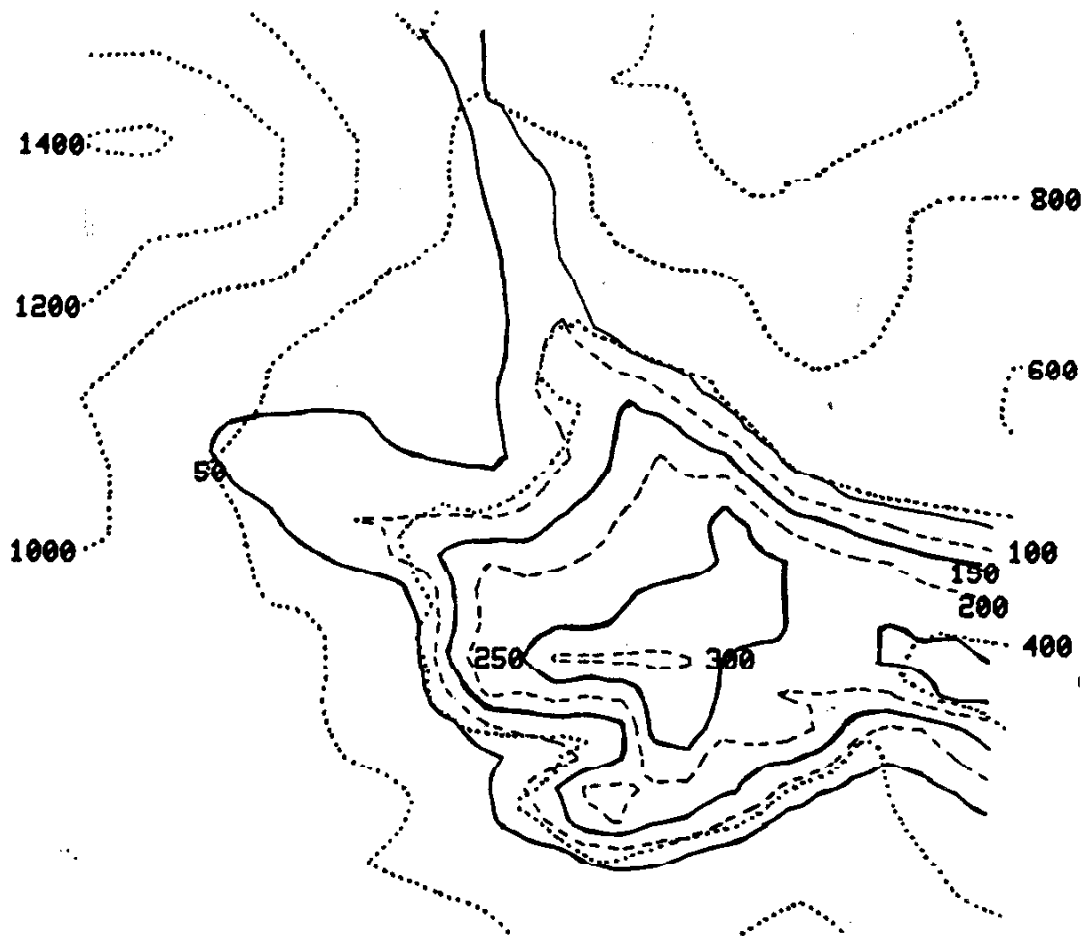
- Fig. 14 Predicted drainage winds over SRP area after 2 hr (a), 4 hr (b), and 8 hr (c) of simulated time. Note shift from katabatic flow into the Savannah River Valley (a) to organized drainage flow later in the simulation (b,c). Simulation started from an atmosphere at rest. Wind vectors are spaced at 2 km intervals with a full feather representing 1 m/s and a half feather 0.5 m/s.
- Fig. 15 Observed winds during night of 27-28 January 1982 at SRP when drainage winds formed along river valley. Wind instrument at Tower C was not functioning. Full feather represents 4.5 m/s; half feather represents 2.25 m/s. Fig. 17a shows well-mixed, neutral conditions at sunset. Drainage winds form and deepen at D towers during night, with 10 m (D1) tower affected first (b,c) and then 61 m (D2) tower (d).



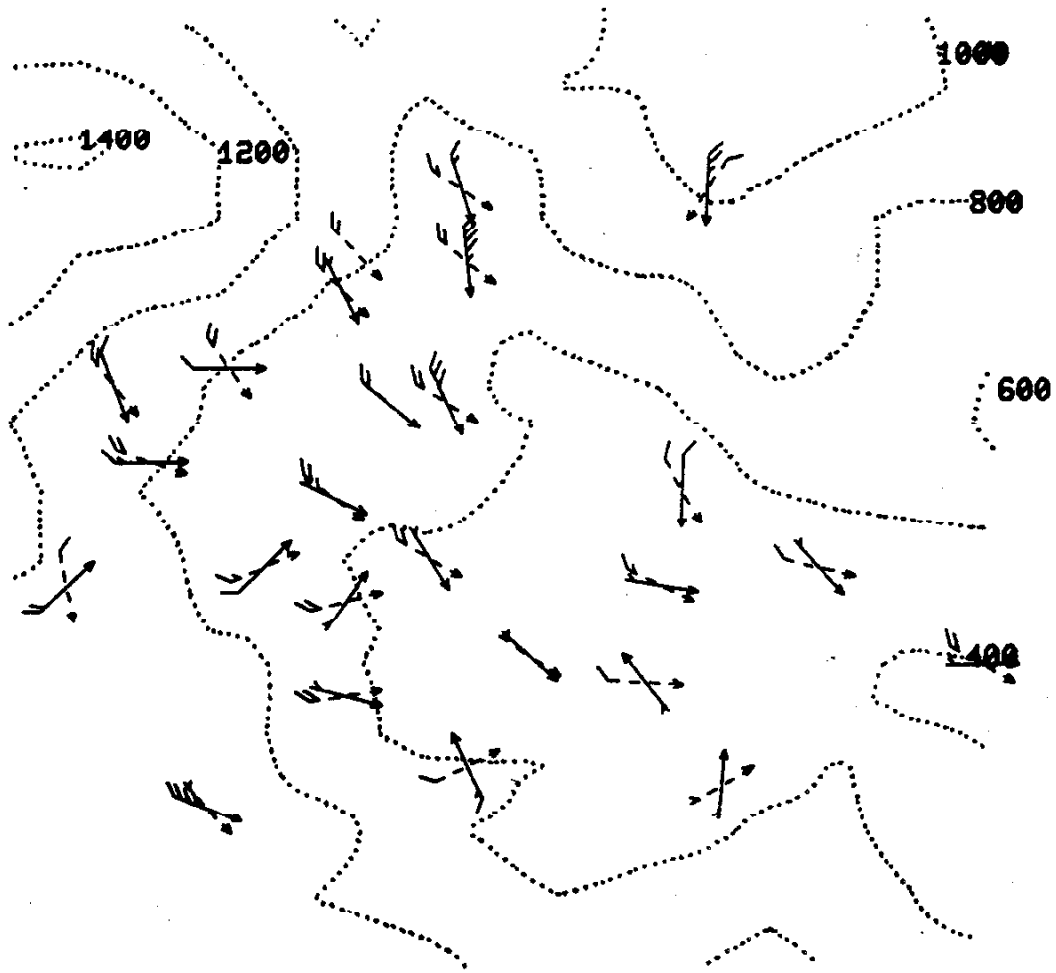




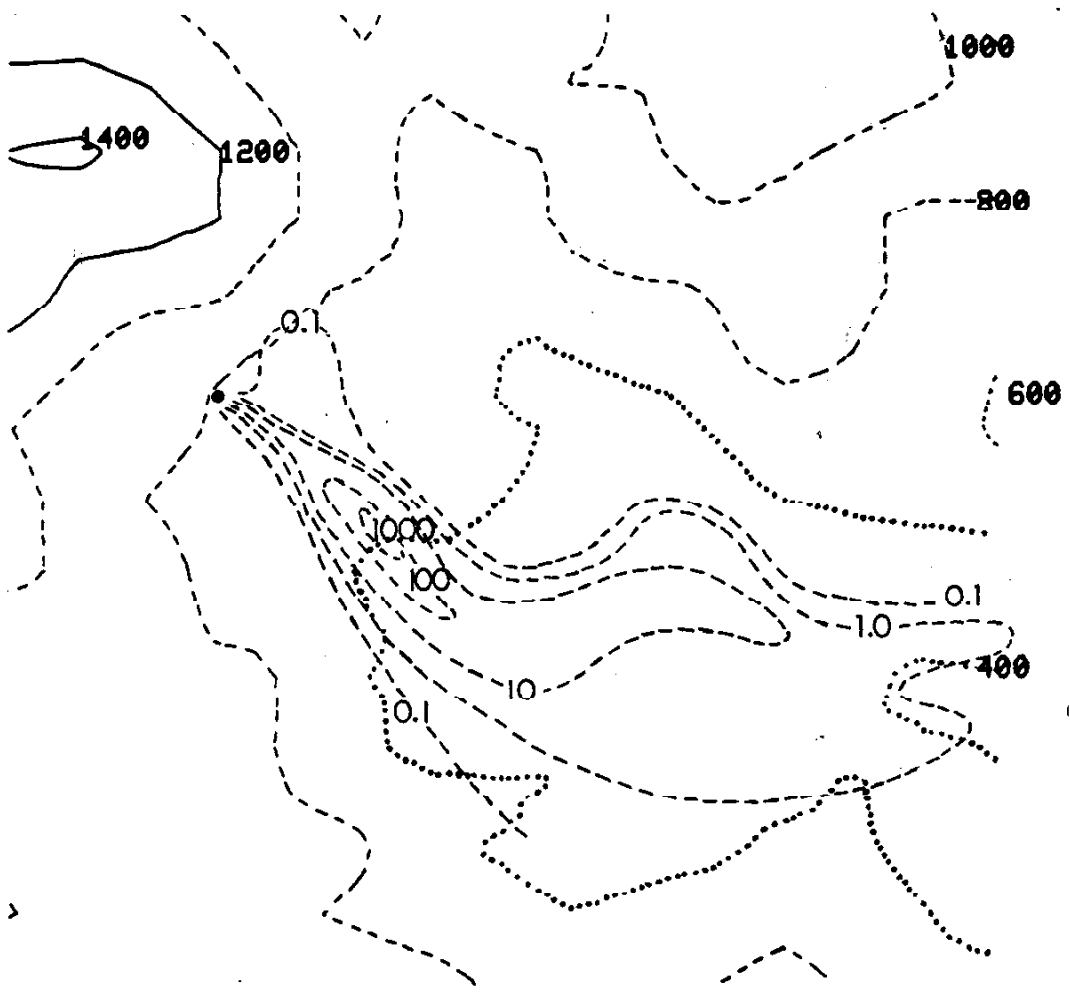
3



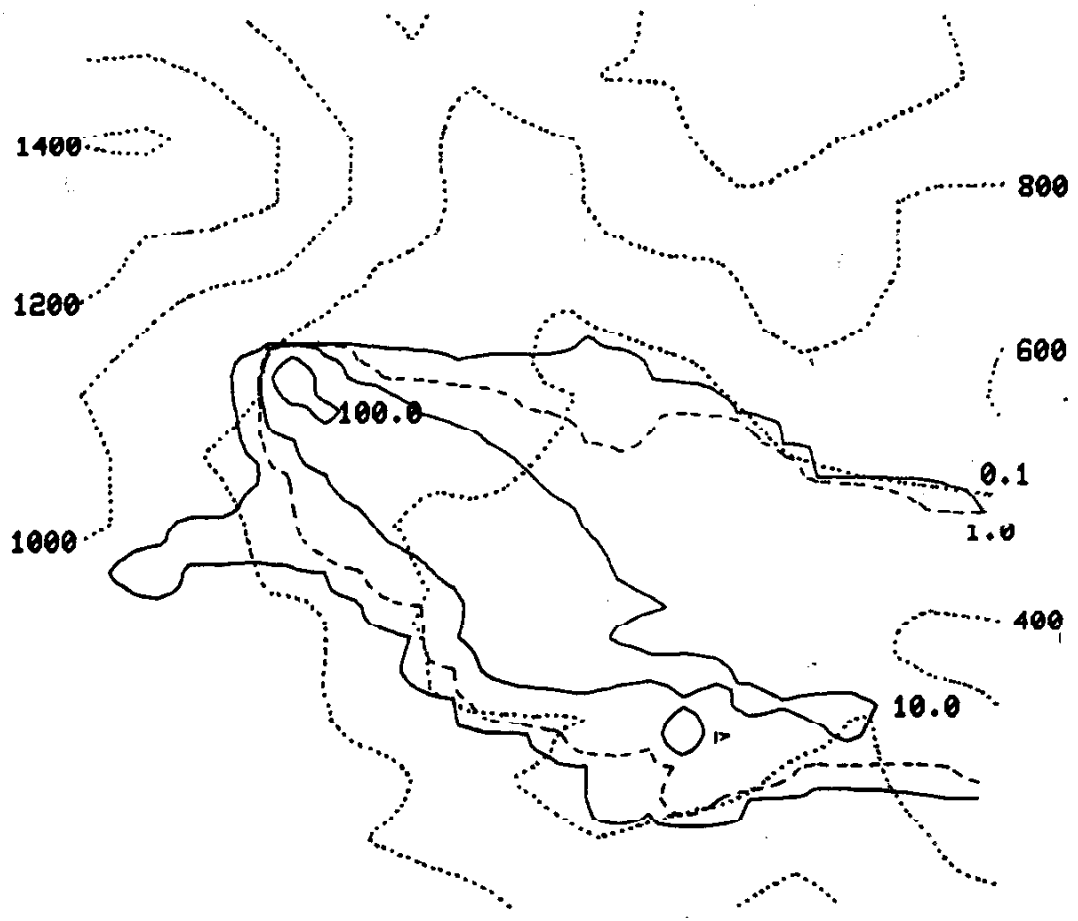
4



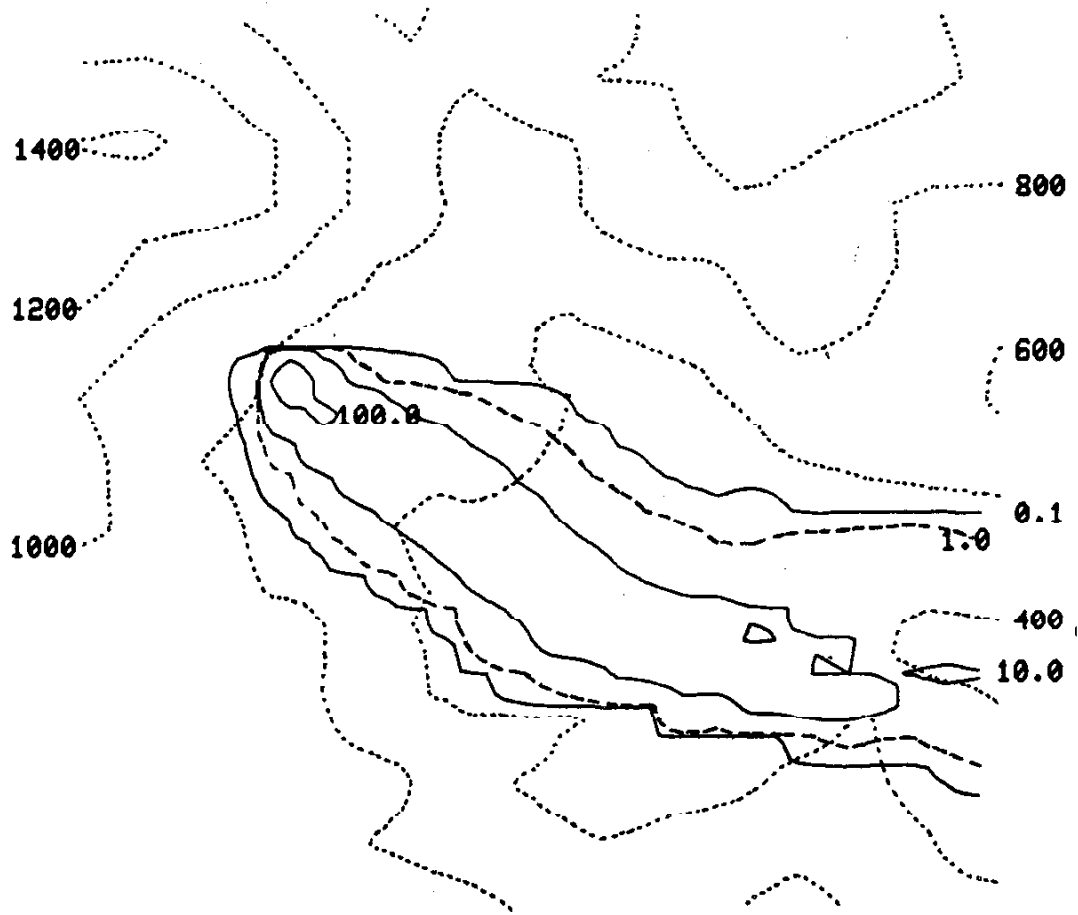
5



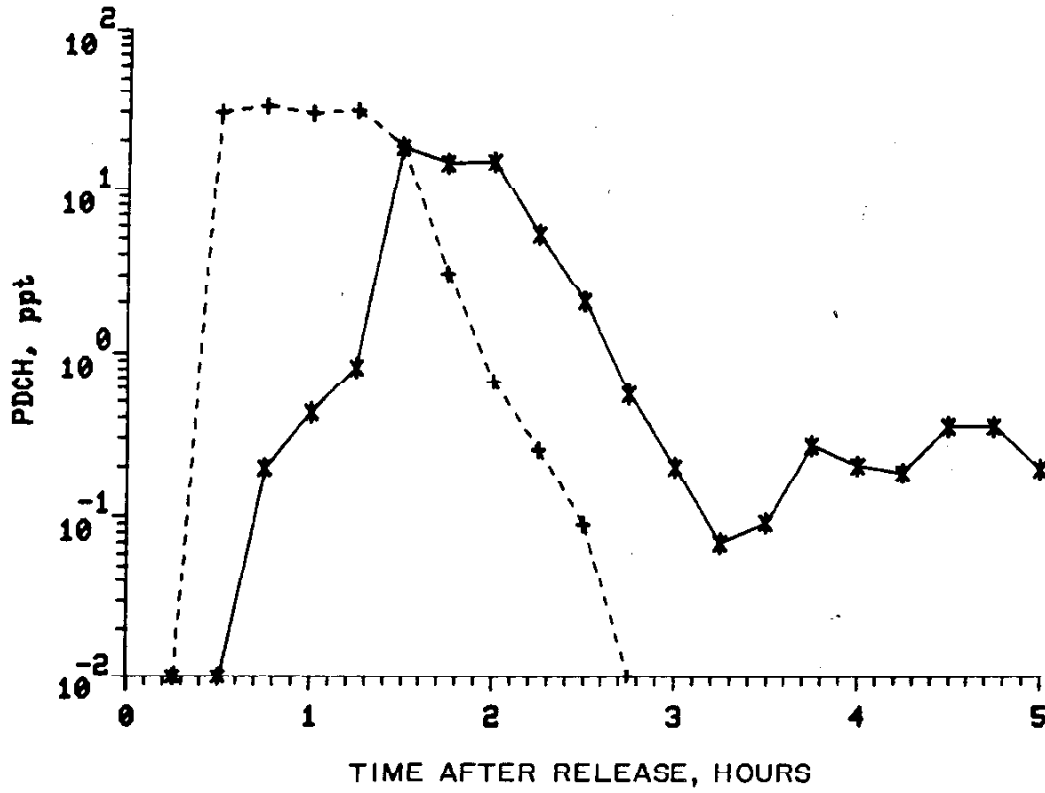
6a



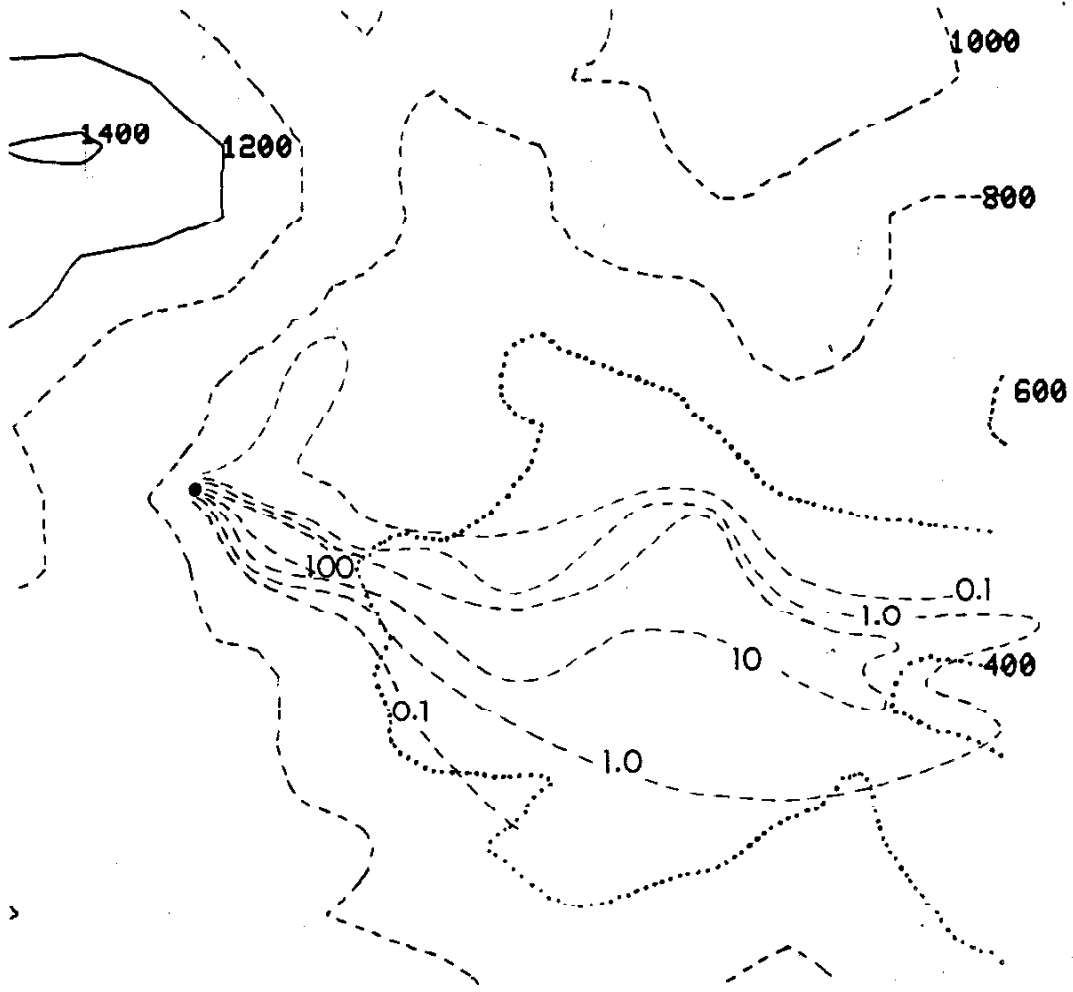
6b



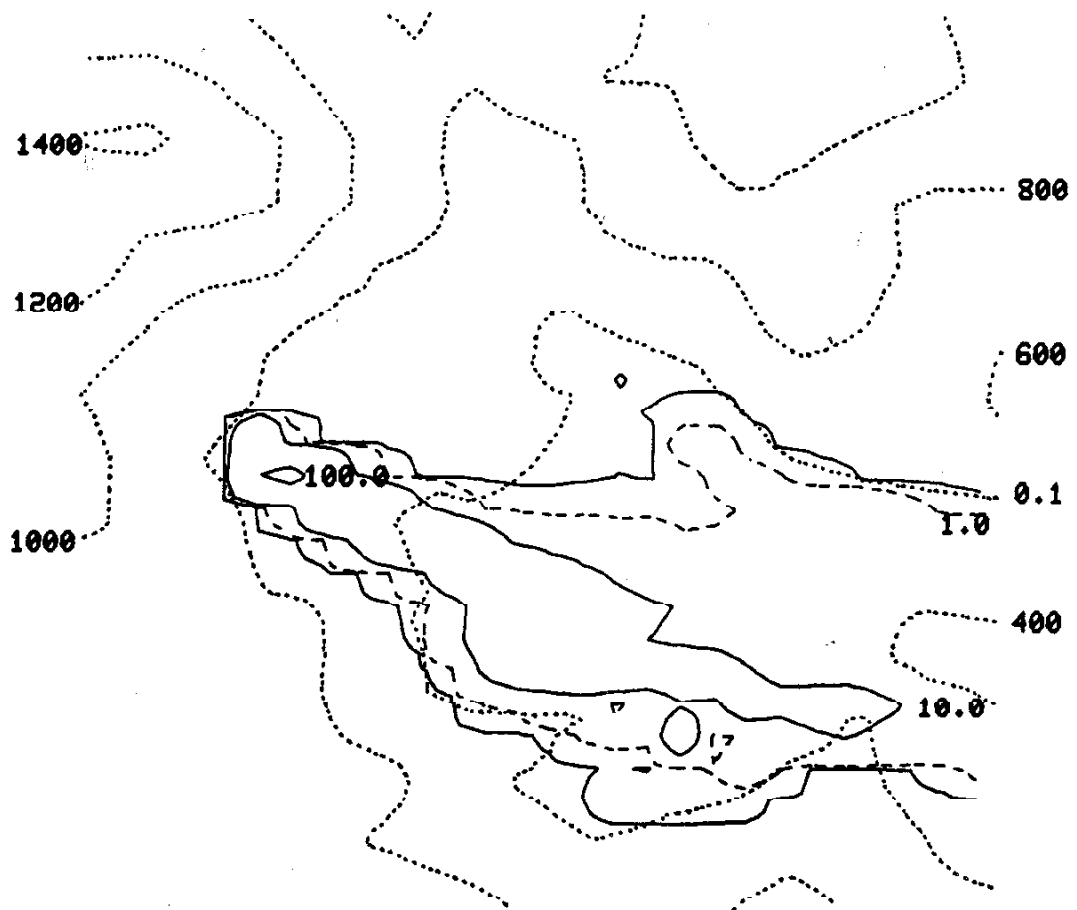
6c



7

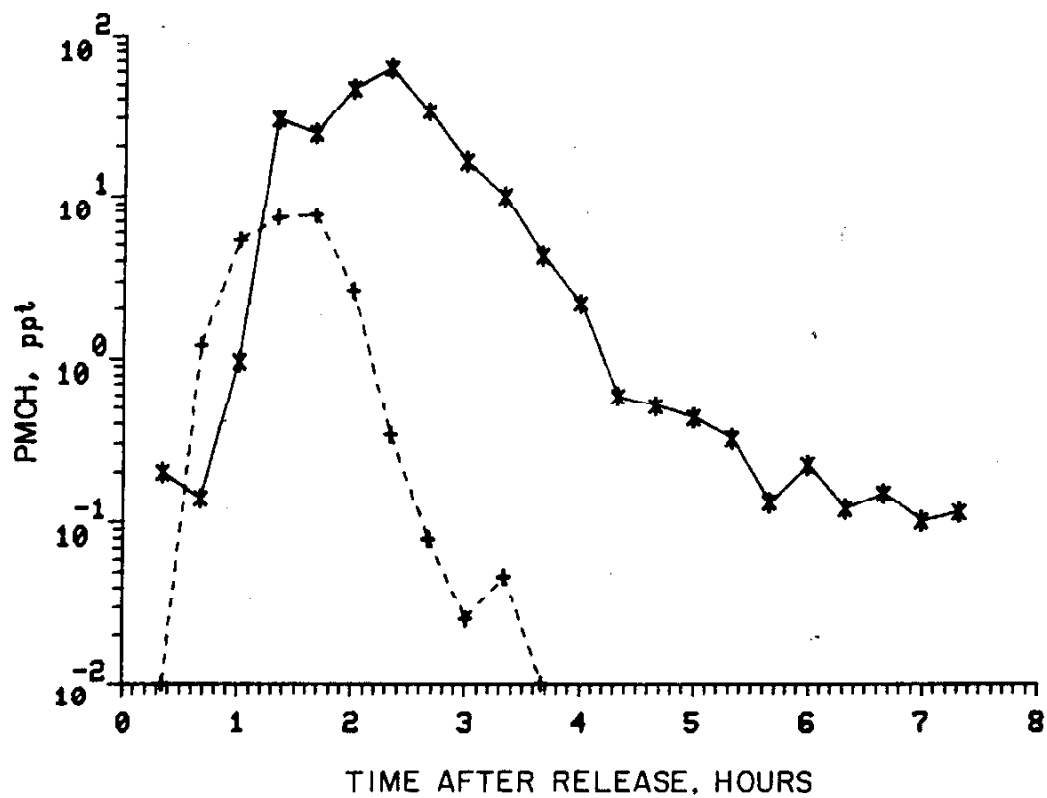


8a

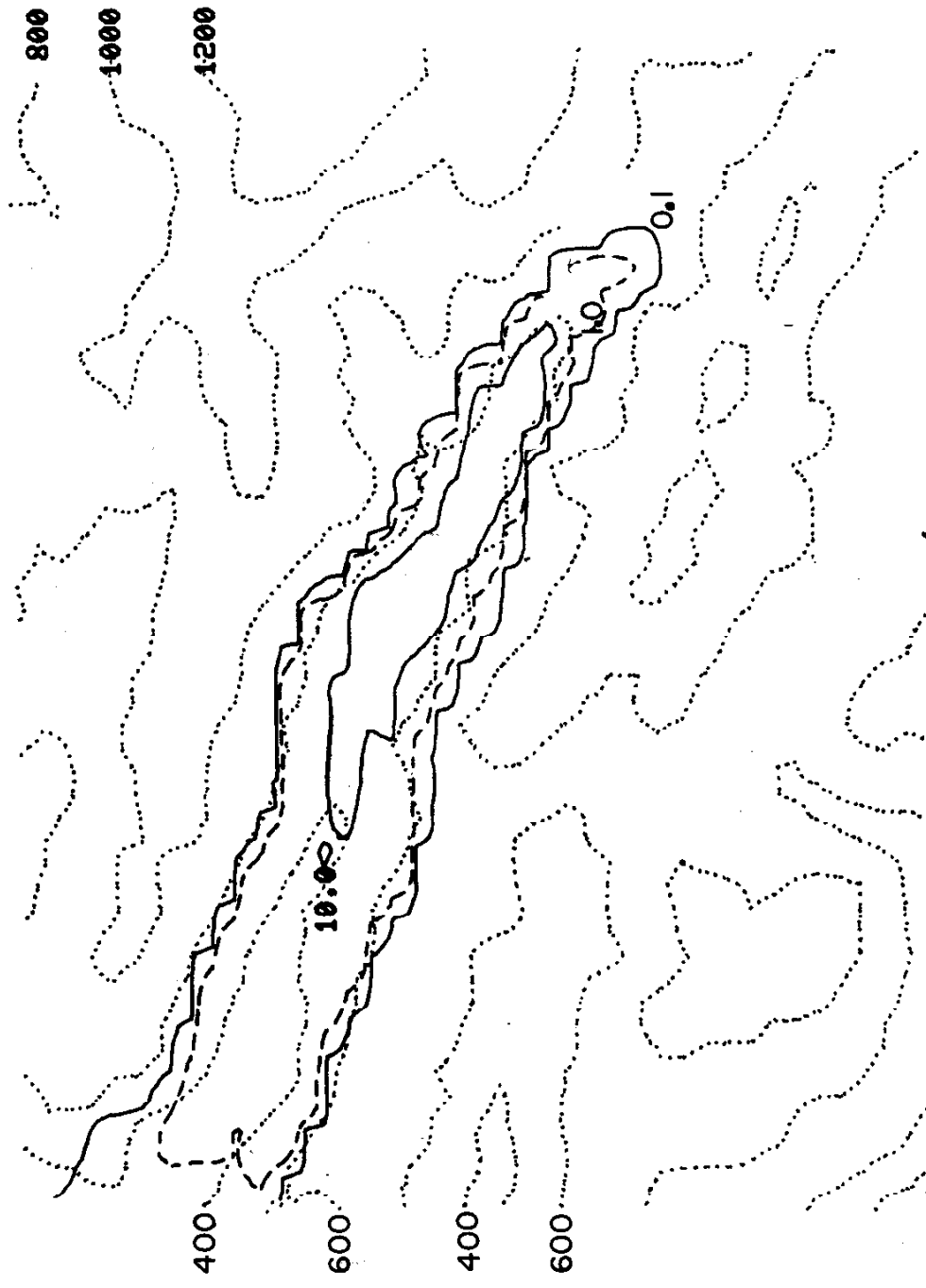


8b

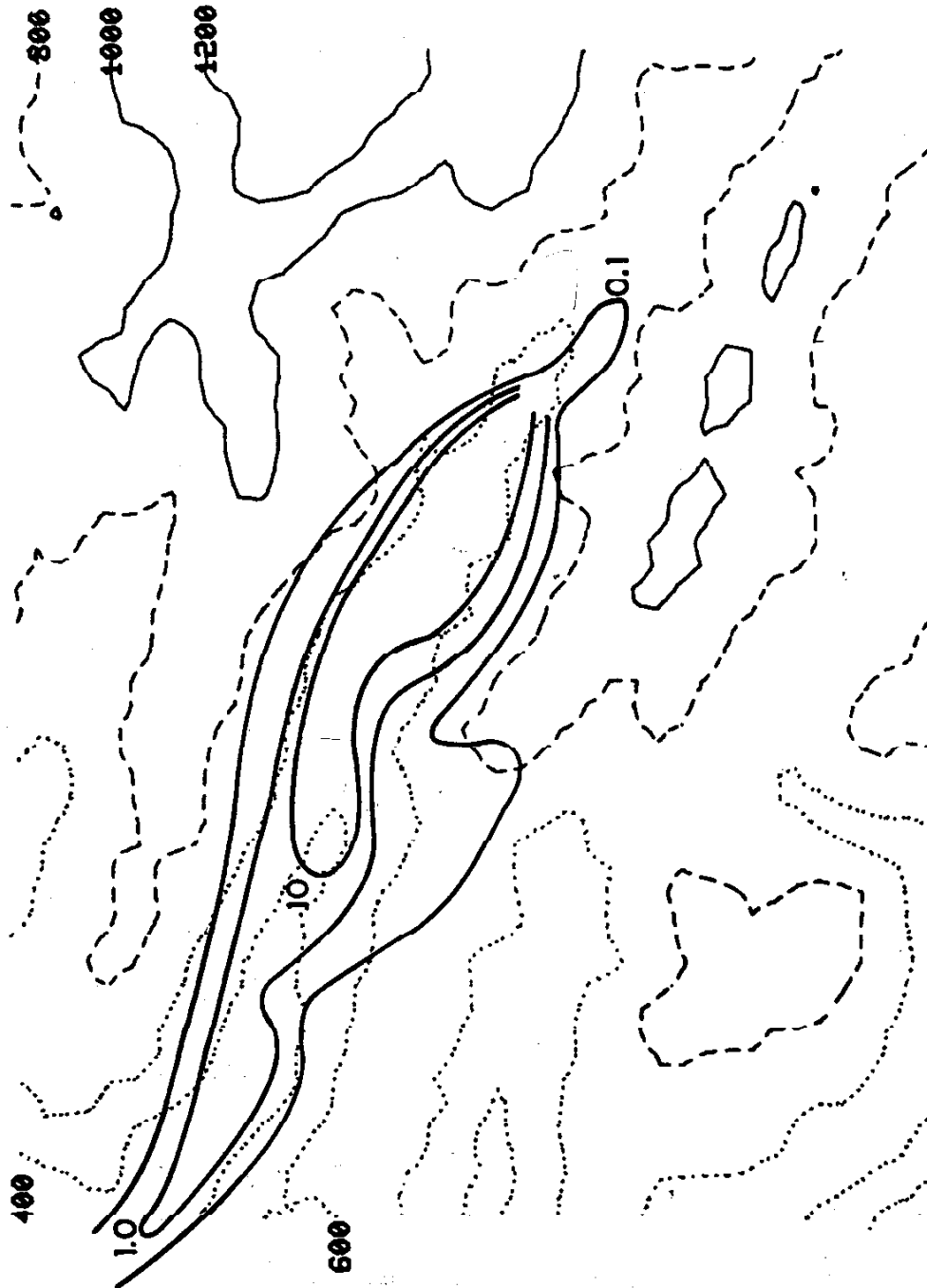
ALL INFORMATION CONTAINED HEREIN IS UNCLASSIFIED

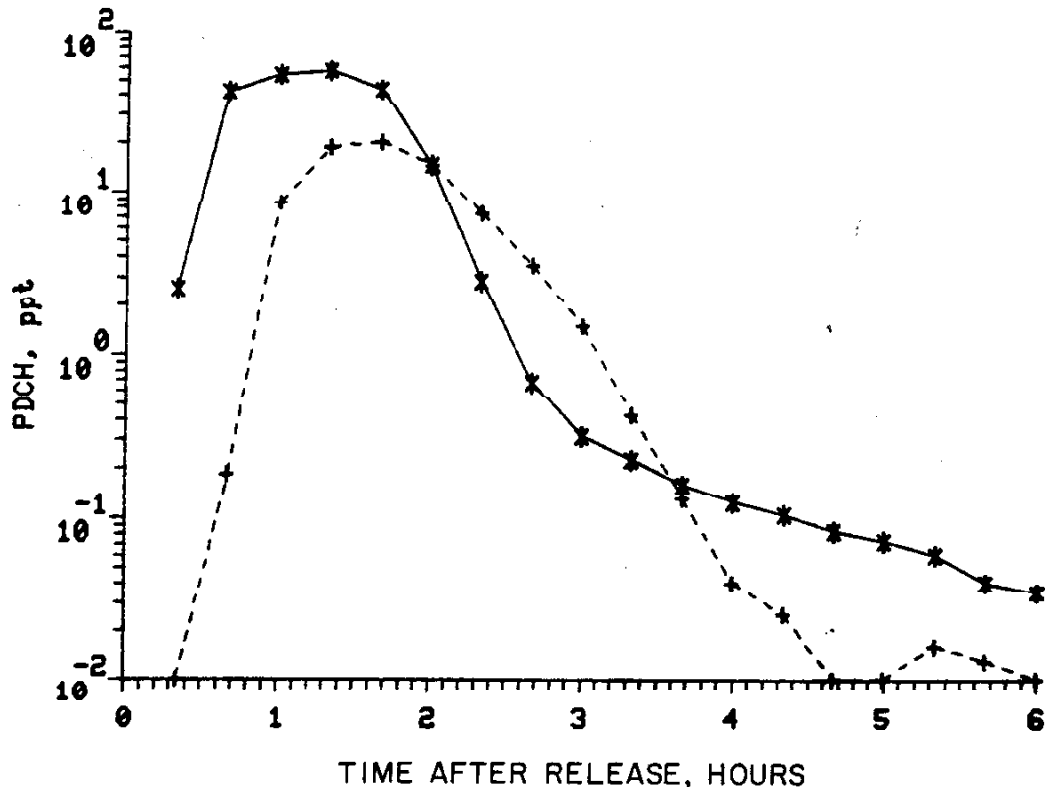


9



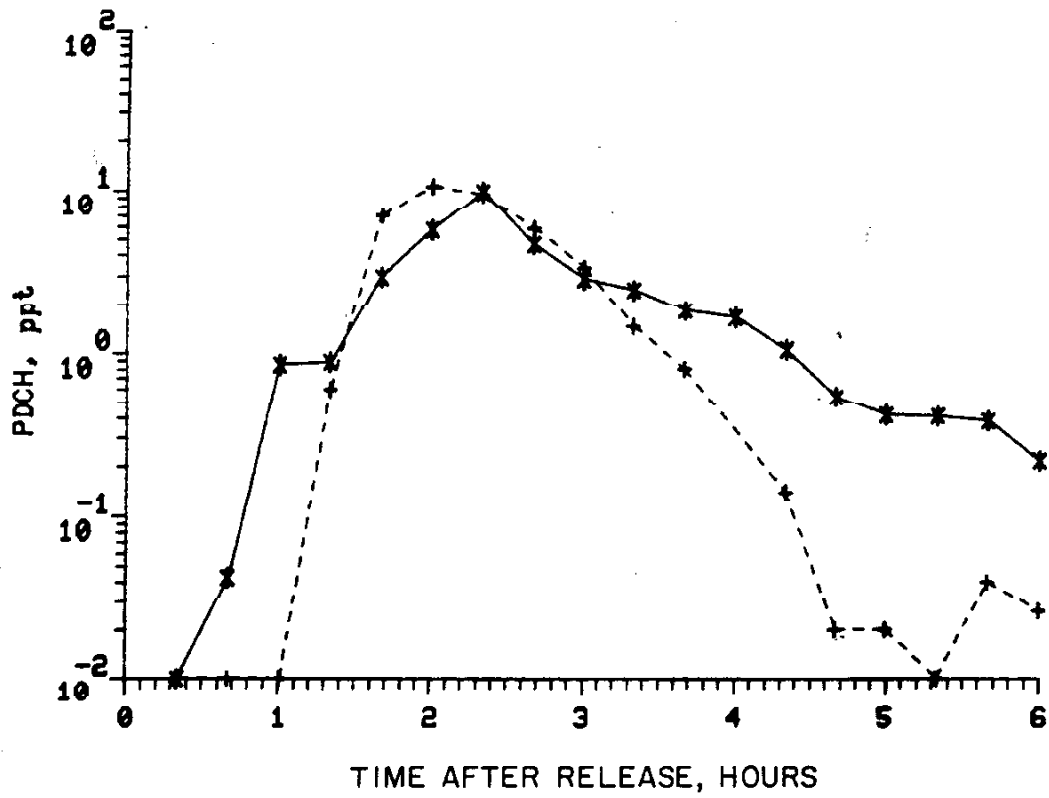
10 a





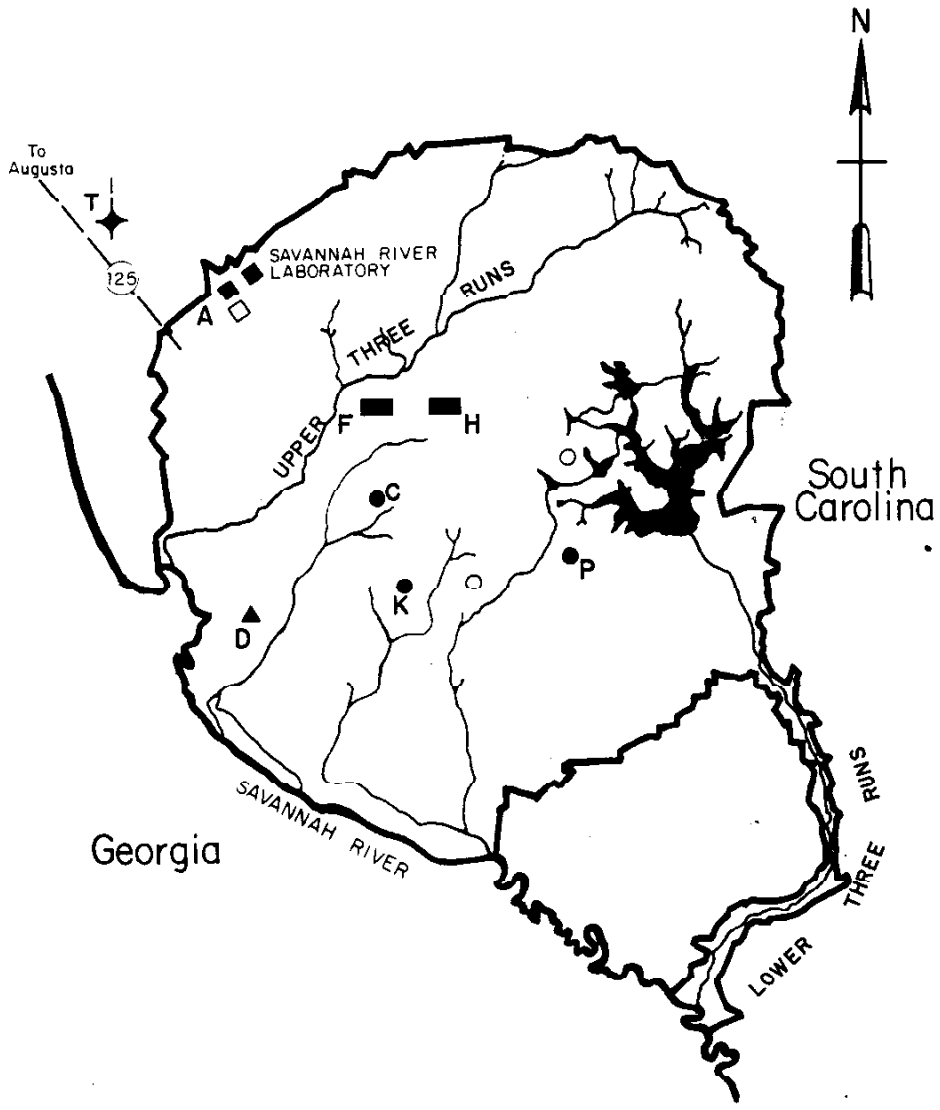
F-11

F-11

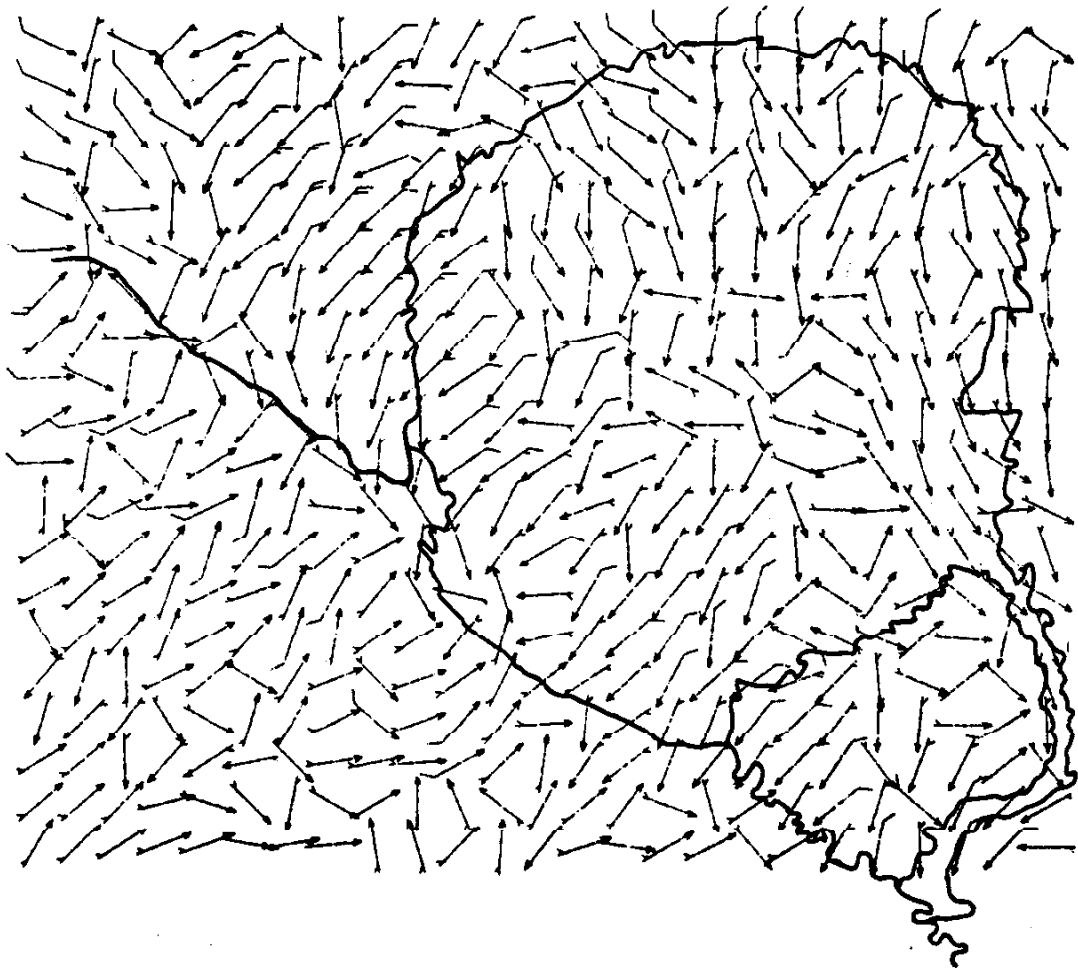


~~17~~

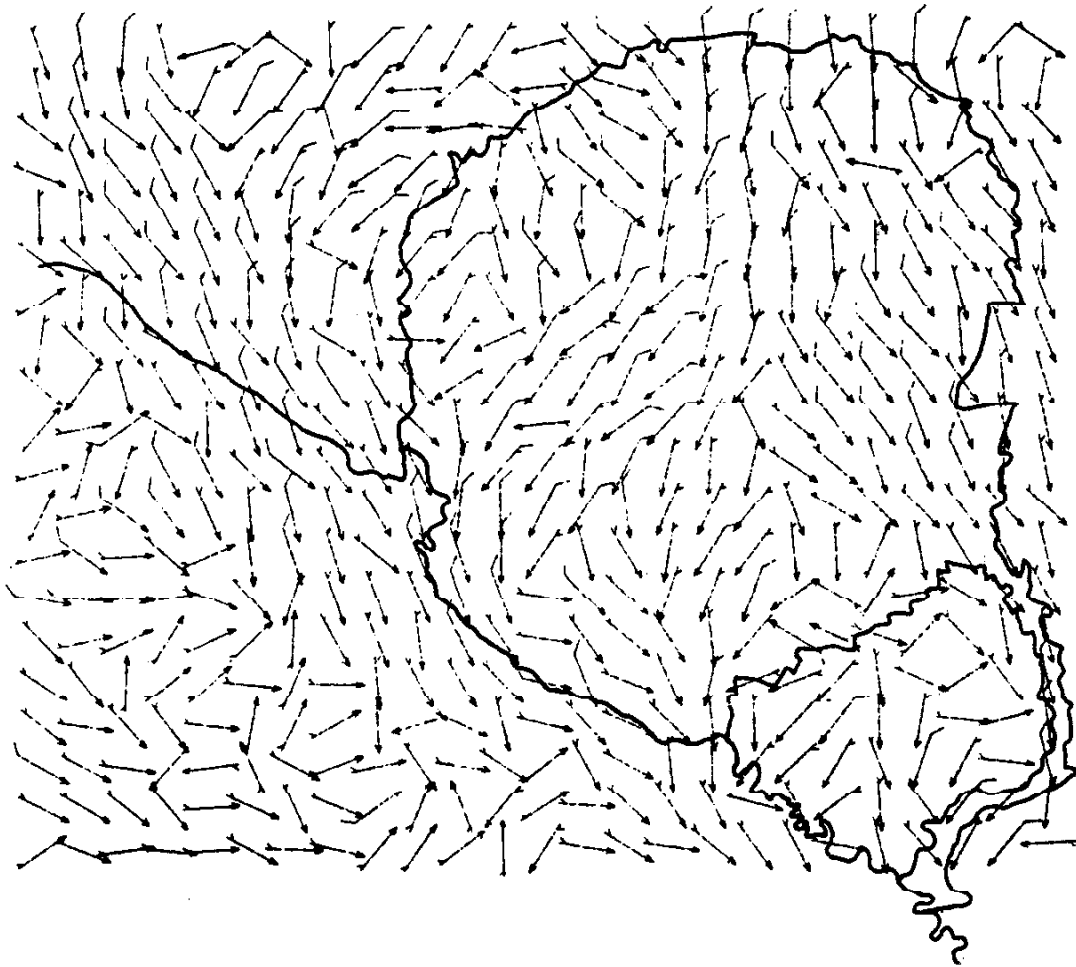
F-12



~~K-15~~

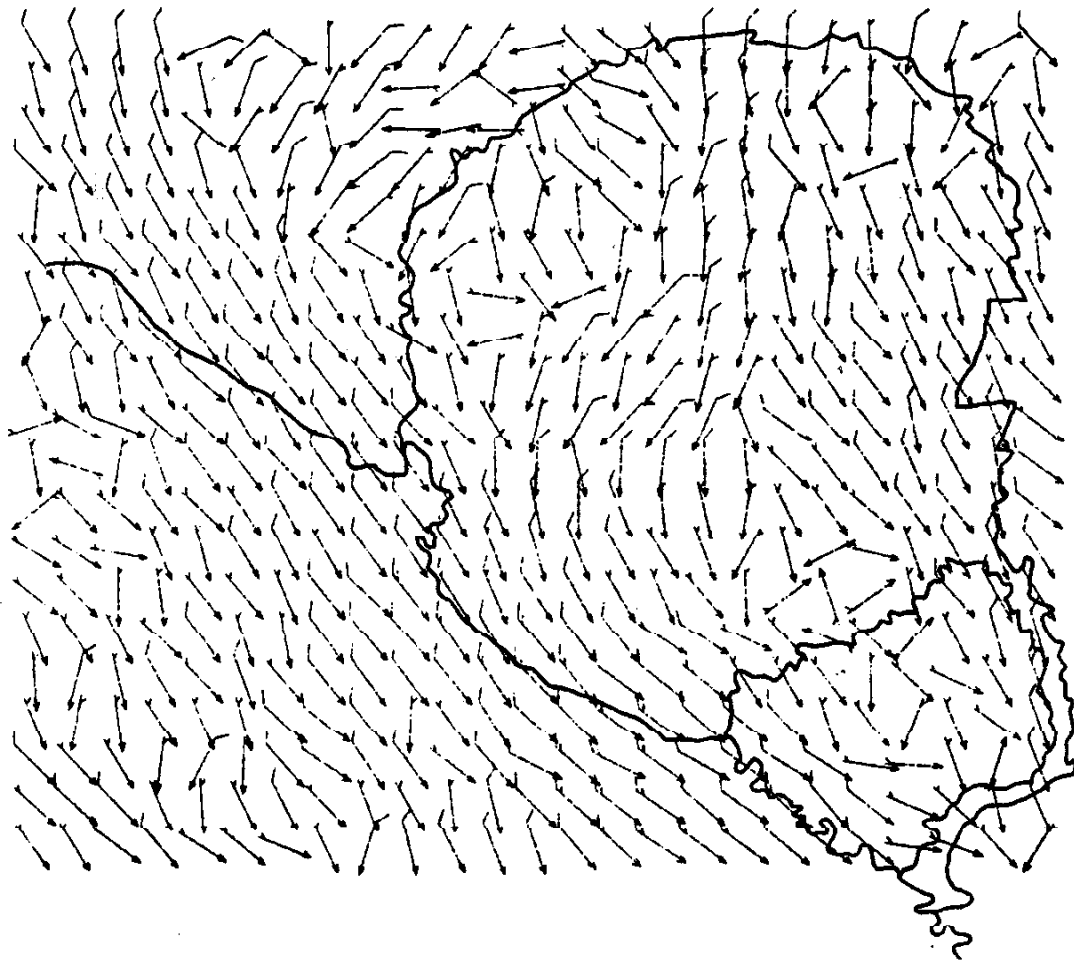


~~100~~



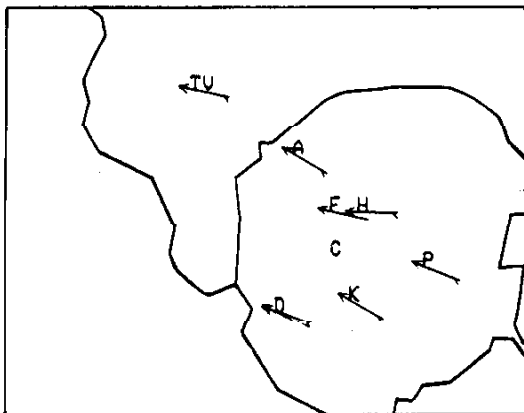
~~8768~~

F-14b

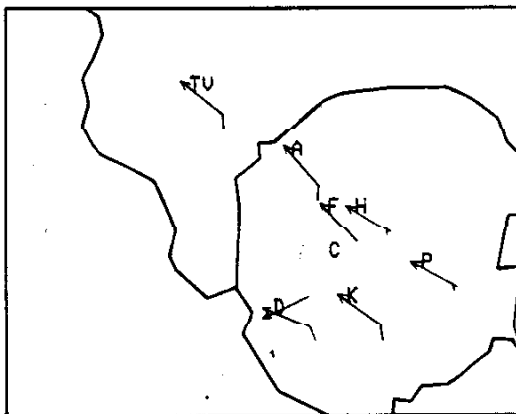


~~160~~

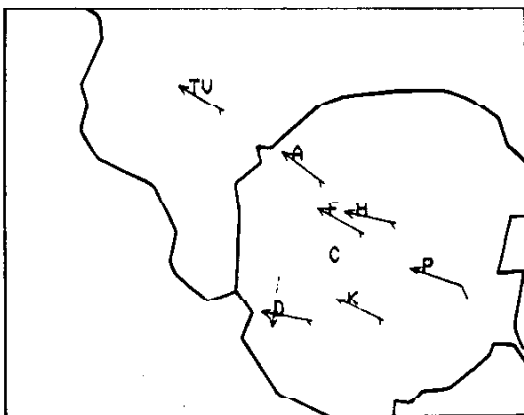
15a



15b



15c



15d

